REPORT DOCUMENTATION PAGE

Form Approved
OMB No. 0704-0188

1. AGENCY USE ONLY (Leave blank)	2. REPORT DATE	3. REPORT TYPE AND DATES COVERED
	22 OCT 96	FINAL

4. TITLE AND SUBTITLE
Control of Leading-Edge Vortices with Suction

5. FUNDING NUMBERS
F49620-93-1-0516
AFOSR-TR-96 0056

6. AUTHOR(S)
Ismet Gursul

7. PERFORMING ORGANIZATION NAME(S) AND ADDRESS(ES)
University of Cincinnati
Dept. of Mechanical, Industrial & Nuclear Engineering, Cincinnati OH 45221

9. SPONSORING / MONITORING AGENCY NAME(S) AND ADDRESS(ES)
AIR FORCE OFFICE OF SCIENTIFIC RESEARCH
DIRECTORATE OF AEROSPACE SCIENCES
BOLLING AFB, DC 20332-6448
NA

10. SPONSORING / MONITORING AGENCY REPORT NUMBER
F49620-93-1-0516

11. SUPPLEMENTARY NOTES

12a. DISTRIBUTION / AVAILABILITY STATEMENT
APPROVED FOR PUBLIC RELEASE
DISTRIBUTION IS UNLIMITED

12b. DISTRIBUTION CODE

13. ABSTRACT (Maximum 200 words)

Several control techniques have been applied in order to control leading-edge vortices at high angle of attack. The purpose of these control techniques is to influence the strength and structure of the vortices, to generate rolling moment, and to delay vortex breakdown.

Since the vorticity of the leading-edge vortices originates from the separation point along the leading-edge, control of development of the shear layer has been chosen as a control strategy in several investigations: blowing and suction in the tangential direction along a rounded leading-edge (Wood et al., 1990; Gu et al., 1993).

14. SUBJECT TERMS			15. NUMBER OF PAGES 47
			16. PRICE CODE
17. SECURITY CLASSIFICATION OF REPORT	18. SECURITY CLASSIFICATION OF THIS PAGE	19. SECURITY CLASSIFICATION OF ABSTRACT	20. LIMITATION OF ABSTRACT
UNCLASSIFIED	UNCLASSIFIED	UNCLASSIFIED	

NSN 7540-01-280-5500

Standard Form 298 (Rev. 2-89)

CONTROL OF LEADING-EDGE VORTICES WITH SUCTION

FINAL TECHNICAL REPORT

Grant No: F49620-93-1-0516

Period Covered: 9/1/94–8/31/96

Prepared for

Air Force Office of Scientific Research
110 Duncan Avenue, Suite B115
Bolling Air Force Base, DC 20332-0001

Prepared by

Ismet Gursul
Assistant Professor
University of Cincinnati
Department of Mechanical, Industrial and Nuclear Engineering
Cincinnati, OH 45221-0072

TABLE OF CONTENTS

1. INTRODUCTION

2. EXPERIMENTAL FACILITIES

3. RESULTS

- **3.1. Surface Suction**
- **3.2. Leading Edge Suction**
- **3.3. Discussion**

4. CONCLUSIONS

REFERENCES

NOMENCLATURE

Appendix A: McCORMICK, S. and GURSUL, I., "Effect of Shear Layer Control on Leading Edge Vortices", *Journal of Aircraft,* in press.

Appendix B: McCORMICK, S. and GURSUL, I. 1996 "Effect of Shear Layer Control on Leading Edge Vortices", AIAA 96-0541, 34th Aerospace Sciences Meeting and Exhibit, January 15-18, 1996, Reno, NV.

1. INTRODUCTION

Several control techniques have been applied in order to control leading-edge vortices at high angle of attack. The purpose of these control techniques is to influence the strength and structure of the vortices, to generate rolling moment, and to delay vortex breakdown.

Since the vorticity of the leading-edge vortices originates from the separation point along the leading-edge, control of development of the shear layer has been chosen as a control strategy in several investigations: blowing and suction in the tangential direction along a rounded leading-edge (Wood et al., 1990; Gu et al., 1993). These studies showed that a rounded, as opposed to a sharp, leading edge can alter the location of separation from the leading edge by tangential blowing. It has been pointed out that this technique uses the Coanda jet effect to help the shear layer attach to the convex surface. Therefore, the application of this technique requires thick rounded leading edges.

Vortex breakdown phenomenon continues to be a challenging aspect of vortical flow fields. Since highly maneuverable aircraft are designed to operate at high angle of attack, vortex breakdown may move onto the wing and affect the stability of the aircraft. The unsteady characteristics (Gursul, 1994; Gursul and Yang, 1995) of the flow field downstream of breakdown are very important for stability and buffeting considerations. It is well known that there are two important parameters which determine the breakdown location: *swirl angle* and *external pressure gradient* outside the vortex core. The principle of any control method is to alter either or both of these parameters. Blowing and suction in the tangential direction along a rounded leading-edge (Wood et al., 1990; Gu et al., 1993) and suction applied around the vortex axis (Werle, 1960; Parmenter and Rockwell, 1990) were shown to delay breakdown. The former is believed to be due to a change in the strength and location of the leading-edge vortices. This is achieved by affecting the location of separation on the rounded leading-edge. Direct control of the separation point modifies the vortex properties such that a reduction in the swirl angle is achieved. The purpose of applying suction around the vortex axis is to

reduce the local adverse pressure gradient, which is achieved by accelerating the axial flow along the core.

One of the objectives of this work is to study the possibility of shear layer control over delta wings with sharp leading edges. In an attempt to control the development of a two-dimensional shear layer, Leu and Ho (1993) applied suction at the trailing edge of a splitter plate. It was shown that the free shear layer is sensitive to the modifications at the origin. The shear layer could be turned to a direction which is about 45 degrees from the streamwise direction. This type of "flow vectoring" was also studied by direct numerical simulations (Hammond and Redekopp, 1994). Gad-el-Hak and Blackwelder (1987) applied periodic perturbations of injection and suction along the leading-edge of a delta wing. They found maximum changes in the evolution of the shear layer when the frequency of perturbations is the subharmonic of the frequency of Kelvin-Helmholtz instability. However, no results were reported regarding the structure of the main vortex and the effect on vortex breakdown. In this work, motivated by previous results, a similar shear layer control technique is explored over a delta wing with sharp leading edges. Suction is applied along the leading edge of a delta wing through a slot (see Figure 1a), and it is shown that the separated shear layer can be effectively manipulated. This, in turn, causes large modifications in the structure of the leading edge vortices. At large angle of attack, vortex breakdown can be controlled as well. It is shown that application of the leading edge suction technique does not require thick rounded leading edges. Control of vortices can be achieved without the use of the Coanda jet effect.

The second objective of this work is to explore the feasibility of vortex control by using suction via a slit on the upper surface of a delta wing (see Figure 1b). It is expected that the leading edge vortex can be maintained in a stable position closer to the wing surface. Depending on the location and magnitude of the suction, the location and strength of the leading edge vortex can be controlled. Independent control of the pair of vortices over delta wings can be used for roll authority. Since the strength and location of the vortices can be altered, this can be used to alter the swirl angle and streamwise pressure gradient, which are known to be the main parameters affecting the vortex

breakdown. Thus, there is a potential for the proposed method to delay vortex breakdown over stationary and unsteady wings.

2. EXPERIMENTAL FACILITIES

Preliminary flow visualization experiments were carried out in a wind tunnel with a cross sectional area of 305 mm by 305 mm. The turbulence intensity in the wind tunnel was 0.25%. Both the leading edge suction and surface suction were tried on the model delta wings (see Figure 1), which had a sweep angle of Λ=65°. The maximum blockage ratio was 3%. The Reynolds number was around Re=12,000. Smoke injected near the apex helped to visualize the vortex core and provided information on vortex breakdown location.

The majority of the experiments were carried out in a water channel with a cross-sectional area of 610 mm by 610 mm (see Figure 2). The turbulence intensity in the water channel is 0.6%. For leading-edge suction, experiments were carried out for two different types of model delta wings (called Model A and B). In the water channel experiments, delta wings with sweep angles Λ=65° and 70° were tested. In Figure 3, the model delta wings are shown for Λ=70°. Model A is the basic delta wing, while Model B has a shorter upper plate which is parallel to the leading edge. At the trailing edge of the wing, the span of the upper plate is 93.4% of the semispan. Since the shear layer turns inboard over the upper surface of the wing for the conventional wings, it was decided to study other configurations for which the upper plate is shorter and is not expected to interfere with the curved shear layer. A third configuration which is similar to Model B was also tested. The span of the upper plate in this model varied linearly with the streamwise distance. The results are very similar to those for Model B (McCormick, 1995). The leading edges were beveled at 45 degrees on the windward side. The height of the suction slot is 1.8 mm. The chord lengths are c=254 mm for Λ=70° and c=203 mm for Λ=65°. The maximum blockage ratio was 5.6%. The Reynolds number based on chord length was in the range of Re=40,000-50,000. The free stream velocity was U_∞=20 cm/sec, and no free surface effects were observed even at the highest angle of attack

(α=42°). The body of the models was made of Plexiglas and the upper plates were made of stainless steel.

Flow visualization of vortex breakdown was done by injecting fluid with food coloring dye near the apex of the models. The flow visualization was videotaped for further analysis. The velocity was measured with a single component laser Doppler velocimetry (LDV) system. The measurement volume was 0.1 mm in diameter and 0.81 mm in length. For axial velocity measurements, the velocity component parallel to the wing surface was measured. Since the measurements were taken parallel to the trailing edge (which is not perpendicular to the vortex axis), the velocity component approximately corresponds to the axial velocity. Also, measurements of the velocity component normal to the wing surface were taken in the plane containing the vortex core axis. As the measurements were taken along a traverse line parallel to the wing surface, the normal velocity approximately corresponds to the swirl velocity across the vortex core. The traversing system used a minimum step of 1 mm which translated to a grid resolution of $\Delta y/s=\Delta z/s=0.0175$ at $x/c=0.6$. The measurement uncertainties for breakdown location and mean velocity were estimated as 0.4% and 1%, respectively.

The suction flow was generated by a pump or fan (for water channel and wind tunnel experiments) located outside the test section (see figure 4). The volume flow rate for suction was measured by a rotameter type flow meter. Further information regarding the experimental setup and instrumentation can be found in McCormick (1995).

3. RESULTS

3.1. Surface Suction

Figure 5 shows flow visualization pictures with suction at $y_s/s=0.7$ for a suction coefficient of $C_\mu=0.72$ and without suction for $\alpha=25°$. It is seen that vortex breakdown location moves downstream with suction. The Reynolds number was Re=14,000. At higher speeds, flow visualization was not clear. In this case, a hot-wire signal was used to detect vortex breakdown. Figure 6 shows, for Re=35,000, hot-wire signals for a location ($x/c=0.8$, $y/s=0.3$, $z/s=0.22$) with and without suction. It is seen that large scale

quasi-periodic motion is suppressed with suction, because the location of vortex breakdown moves downstream. The exact location of vortex breakdown was difficult to determine because of limitations of flow visualization. However, based on the hot-wire signals, the vortex breakdown location moved to a downstream location $x_{bd}/c>0.8$, since the probe was located at x/c=0.8.

The effect of location of suction slot is shown in Figure 7, together with the results for the leading edge suction. It is seen that, as the suction slot gets closer to the leading edge, suction becomes more effective in delaying vortex breakdown. However, surface suction is less effective than the leading edge suction.

3.2. Leading Edge Suction

From the wind tunnel experiments for $\Lambda=65°$, the variation of breakdown location with suction coefficient is shown in Figure 8 for Models A and B. The fundamental difference in the response of Models A and B is that the breakdown location moves downstream for Model A whereas the breakdown location moves upstream for Model B. For Model A, vortex breakdown location could be delayed up to 40% of the chord length. When compared with the results by Gu et al. (1993), this maximum improvement is nearly the same. Also, for Model A, the breakdown location reaches a nearly constant level at larger values of the suction coefficient. Although suction causes the vortex core to get closer to wing surface for both models, the location of the vortex core changes slightly with the suction coefficient for Model A while there is a large change of core location with small amounts of suction coefficient for Model B (McCormick, 1995). In fact, similar amounts of change in the core location can be obtained with suction coefficients that are one order of magnitude smaller for Model B than for Model A.

From the water channel experiments for $\Lambda=70°$, the variation of breakdown location with suction coefficient is shown in Figure 9 for Models A and B. The results are qualitatively similar to those presented in Figure 8. For Model A, the effect of suction on breakdown is generally positive, except at very large angles of attack where suction does not make much difference. For $\alpha=30°$, the breakdown location reaches a

maximum around C_μ=0.024 after which it becomes nearly constant. Detailed LDV measurements were carried out for α=30°.

The constant contours of the normalized time-averaged axial velocity for x/c=0.6 (upstream of the breakdown location) are compared in Figure 10 for C_μ=0 and C_μ=0.024 at which the breakdown location is at maximum downstream location. It is clear that the vortex core moves inboard and closer to the wing surface. There is also a slight decrease in the maximum axial velocity with suction. The constant contours of the normalized rms axial velocity are compared in Figure 11 for C_μ=0 and C_μ=0.024. The shape of the rms velocity contours is a good indicator of the shear layer and main vortex. (This was also shown for vortical flows over a body of revolution at incidence (Degani, 1991). The high rms velocity fluctuations indicated the location of the vortex cores. The rms velocity contours were found to be representative of the cross sections of the tip vortices). In the present experiments, very large levels of rms velocity (up to 30% of the free stream velocity) in the shear layer and in the core of the leading edge vortex were observed. It should be noted that this high rms velocity level is observed well upstream of the breakdown location. Other experiments in vortical flows (in the absence of breakdown) showed very high levels of rms velocity (Degani 1991; Schmucker and Gersten 1988; Cornelius 1995). This is not very surprising if the dynamics of the shear layer is considered (i.e., development of coherent structures and pairing etc.). Although high level of rms velocity was reported in the vortex cores previously for large Reynolds numbers, the existence of high levels was not known for relatively low Reynolds numbers (based on the chord length) such as Re=50,000. It is clear from Figure 11 that, with suction, the direction of the shear layer is changed. It is also evident that the vortex core moves inboard and toward the wing surface with suction.

In order to quantify the effect of suction on upstream conditions (before breakdown) and on the parameters affecting breakdown, detailed measurements were taken at x/c=0.6 for several values of the suction coefficient. The location of vortex core was found by locating the position of the maximum of the axial velocity distribution (at x/c=0.6, upstream of breakdown location). Then, measurements of axial and swirl velocity components were taken across the vortex core. The variation of location of the

vortex core is shown in Figure 12. It is seen that the vortex core moves slightly inboard and closer to the wing surface with increasing suction coefficient. However, with increasing suction coefficient, the changes in the core location become relatively small. The variation of axial and swirl velocities across the core is shown in Figure 13. A decrease in the maximum axial velocity is observed with increasing suction. The maximum values of the swirl velocity also decrease with increasing suction. Slightly outboard of the core, a decrease and then a local maximum are observed (due to the shear layer), followed by a leveling of the swirl velocity. Based on the measured axial and swirl velocity components, the swirl angle ($\phi=\tan^{-1} V/U$) can be calculated as a function of the distance from the vortex axis. The variation of swirl angle with the distance from the vortex axis is given in detail in McCormick (1995). The swirl angle is zero at the center of the vortex core and reaches a maximum at the edge of the subcore (the subcore being the region where most of the streamwise vorticity is confined). The variation of maximum swirl angle with the suction coefficient is shown in Figure 14a. It is seen that there is a decrease in swirl angle with increasing suction coefficient although the changes become more gradual at larger values of the suction coefficient. The axial vorticity distribution can also be calculated assuming rotational symmetry. In other words, the swirl velocity profile is sufficient to estimate the axial vorticity. The axial vorticity component is given by $\omega=\partial V/\partial r+V/r$. An example of the calculated vorticity distribution (by the forward differencing method) is given in McCormick 1995. The maximum axial vorticity (which occurs at the vortex axis) is shown as a function of suction coefficient in Figure 14b. A decrease in the maximum axial velocity with suction is observed. However, there is almost no change with further changes in the suction coefficient. In addition, the variation of circulation (obtained from the velocity measurements along the path shown in inset) is shown as a function of suction coefficient in Figure 14c. The overall circulation decreases with increasing suction coefficient. Although this closed contour encloses the main vortex, secondary vortex, and shear layer, it is a reasonable indicator of the strength of the main vortex. Moreover, the circulation calculated this way can be interpreted as the rate at which vorticity is fed. In summary, it is shown that, for $\alpha=30°$, suction delays the vortex breakdown for Model A. This is due to a decrease in

maximum swirl angle and circulation as well as in maximum axial vorticity. Further experiments for Λ=65° also showed similar results.

For Model B, the flow visualization showed an opposite trend for the variation of breakdown location with suction (see Figure 9). Therefore, it was decided to carry out detailed measurements for Model B at α=20°. The constant contours of the normalized time-averaged axial velocity for x/c=0.6 (upstream of the breakdown location) are compared in Figure 15 for C_μ=0 and C_μ=0.0027. It is seen that an extremely small amount of suction (almost one-tenth of the amount used for Model A) is sufficient to displace the vortex core. There is a slight increase in the maximum axial velocity. The constant contours of the normalized rms axial velocity shown in Figure 16 indicate that the vortex core moves outboard and closer to the wing surface with suction. Higher levels of rms axial velocity are found in the core when suction is applied.

The location of vortex core was found from the axial velocity distributions (at x/c=0.6, upstream of breakdown location). From the measurements of the axial and swirl velocity components, several parameters were estimated. The variation of maximum swirl angle with the suction coefficient is shown in Figure 17a, which reveals a slight increase with increasing suction. The maximum axial vorticity (at the vortex axis) is shown as a function of suction coefficient in Figure 17b, which indicates an initial increase followed by a slight decrease with increasing suction coefficient. In addition, the variation of circulation (obtained from the velocity measurements along the path shown in inset) is shown as a function of suction coefficient in Figure 17c. This shows that overall circulation is not affected much with suction. In summary, for α=20°, suction causes premature vortex breakdown for Model B. This is due to an increase in maximum swirl angle and maximum axial vorticity.

3.3. Discussion

Experiments using Model A show that breakdown can be effectively moved downstream when suction is applied. Suction allows the shear layer to be manipulated at the point of separation along the leading edge. In this way, not only can the shear layer be "vectored" inboard and toward the wing surface, but also some of the vorticity can be

removed before it enters the vortex core. This decrease in vorticity also causes the circulation and swirl angle to decrease. As a result, the vortex breakdown location moves downstream.

Experiments using Model B show that breakdown moves upstream when suction is applied. Unlike Model A, Model B has the suction slot ("sink") located inboard, away from the separated shear layer (see Figure 3). The shear layer has already separated and begun its characteristic curvature over the wing surface before the suction slot of Model B is encountered. This allows the vortex core to be manipulated while removing very little, if any, vorticity from the shear layer. Therefore, the vorticity fed into the shear layer does not change with suction. However, the shear layer can still be "vectored" inboard in a very effective way (with very small suction). The swirl velocity increases slightly as the separating shear layer is pulled tangentially by suction. The axial velocity component experiences very little change. The increasing swirl velocity component causes an increase in swirl angle which causes the breakdown location to move upstream.

4. CONCLUSIONS

The effect of suction on the wing surface as well as along the leading edge on vortex breakdown has been investigated. Suction has been found to be more effective in delaying vortex breakdown for suction slots closer to the leading edge. However, surface suction is less effective than the leading edge suction.

The effect of leading edge suction on leading edge vortices over delta wings with sharp leading edges was investigated. By using suction near the separation point, the orientation of the shear layer could be modified. As a result, the structure of the leading edge vortex and its location over the wing were modified as well. The maximum swirl angle in the core and overall circulation decreased with increasing suction. This caused the vortex breakdown location to move downstream. The geometry of the suction slot along the leading edge was found to be important. Use of a shorter plate on the upper surface of the wing caused the breakdown location to move upstream with suction. However, in this case, extremely small amounts of suction caused the location of the leading edge vortex to change dramatically. This can be used to generate rolling moment

over a delta wing. The leading edge suction technique offers advantages over other methods, such as flaps, by eliminating the need for moving surfaces and complicated mechanism. Thick rounded leading edges are not necessary.

REFERENCES

Cornelius, K.C., "Analysis of Vortex Bursting Utilizing Three-Dimensional Laser Measurements", *Journal of Aircraft,* vol. 32, no.2, February 1995, pp. 297-306.

Degani, D. "Effect of splitter plate on unsteady flows around a body of revolution at incidence", *Physics of Fluids A*, vol. 3, no. 9, September 1991, pp. 2122-2131.

Gad-el-Hak, M. and Blackwelder, R.F., "Control of the Discrete Vortices from a Delta Wing", *AIAA Journal,* vol. 25, no. 8, August 1987, pp. 1042-1049.

Gu, W., Robinson, O. and Rockwell, D., "Control of Vortices on a Delta Wing by Leading-Edge Injection'', *AIAA Journal*, vol. 31, no. 7, July 1993, pp. 1177-1186.

Gursul, I. "Unsteady Flow Phenomena over Delta Wings at High Angle of Attack'', *AIAA Journal,* vol. 32, no. 2, February 1994, pp. 225-231.

Gursul, I and Yang, H., "On Fluctuations of Vortex Breakdown Location", *Physics of Fluids,* vol. 7, no. 1, January 1995, pp. 229-231.

Hammond , D. and Redekopp, L.G., "Global Dynamics and Flow Vectoring in Asymmetric Wakes", AIAA Paper 94-2219, 25th AIAA Fluid Dynamics Conference, June 20-23, 1994, Colorado Springs, CO.

Leu, T-S. and Ho, C-M., "Free Shear Layer Control and its Application to Fan Noise", AIAA Paper 93-3242, AIAA Shear Flow Conference, July 6-9, 1993, Orlando, FL.

McCormick, S., "Effect of Leading-Edge Suction on Vortices over Delta Wings", M.S. Thesis, University of Cincinnati, 1995.

Parmenter, K. and Rockwell, D., "Transient Response of Leading-Edge Vortices to Localized Suction'', *AIAA Journal*, vol. 28, no. 6, June 1990, pp. 1131-1133.

Schmucker, A. and Gersten, K., "Vortex Breakdown and its Control on Delta Wings", *Fluid Dynamics Research*, vol. 3, 1988, pp. 268-272.

Werle, H. "Sur l'eclatement des tourbillons d'apex d'une aile delta aux fibles vitesses'', *La Recherche Aeronautique*, no. 74, January-February 1960, pp. 23-30.

Wood, N.J., Roberts, L. and Celik, Z., "Control of Asymmetric Vortical Flows over Delta Wings at High Angles of Attack'', *Journal of Aircraft*, vol. 27, no. 5, May 1990, pp. 429-435.

NOMENCLATURE

A_s	cross-sectional area of suction slot
c	root chord
C_μ	suction coefficient, $(V_s/U_\infty)^2(A_s/S)$
r	radial distance from vortex axis
Re	Reynolds number
S	Surface area of the wing
s	local semispan
U_∞	free stream velocity
U	time-averaged axial velocity
u_{rms}	rms axial velocity
V	time-averaged swirl velocity
V_s	suction velocity

x	chordwise distance from the apex of the wing
x_{bd}	chordwise location of vortex breakdown
y	spanwise distance from wing root
z	distance above wing surface
α	angle of attack
Γ	circulation
ϕ	swirl angle, $\tan^{-1} V/U$
Λ	sweep angle
ω	vorticity

List of Figures

Figure 1: Schematic of leading-edge suction and surface suction.

Figure 2: Schematic of water channel.

Figure 3: Model delta wings for Λ=70°.

Figure 4: Schematic of suction system.

Figure 5: Flow visualization of vortex breakdown without suction (top) and with suction (bottom), y_s/s=0.7, C_μ=0.72, α=25°, Re=14,000.

Figure 6: Hot-wire signals at (x/c=0.8, y/s=0.3, z/s=0.22) without suction (top) and with suction (bottom), y_s/s=0.7, C_μ=0.72, α=25°, Re=35,000.

Figure 7: Variation of breakdown location as a function of suction coefficient.

Figure 8: Variation of breakdown location with suction coefficient for (a) Model A, (b) Model B, Λ=65°.

Figure 9: Variation of breakdown location with suction coefficient for Models A and B, Λ=70°.

Figure 10: Contours of normalized time-averaged axial velocity for C_μ=0 and C_μ=0.024, Model A, Λ=70°, α=30°, x/c=0.6.

Figure 11: Contours of normalized rms axial velocity C_μ=0 and C_μ=0.024, Model A, Λ=70°, α=30°, x/c=0.6.

Figure 12: Variation of location of vortex core, Model A, Λ=70°, α=30°, x/c=0.6.

Figure 13: Variation of axial and swirl velocity across the core, Model A, Λ=70°, α=30°, x/c=0.6.

Figure 14: Variation of (a) maximum swirl angle (b) maximum axial vorticity (c) circulation with suction coefficient, Model A, Λ=70°, α=30°, x/c=0.6.

Figure 15: Contours of normalized time-averaged axial velocity for C_μ=0 and C_μ=0.0027, Model B, Λ=70°, α=20°, x/c=0.6.

Figure 16: Contours of normalized rms axial velocity C_μ=0 and C_μ=0.0027, Model B, Λ=70°, α=20°, x/c=0.6.

Figure 17: Variation of (a) maximum swirl angle (b) maximum axial vorticity (c) circulation with suction coefficient, Model B, Λ=70°, α=20°, x/c=0.6.

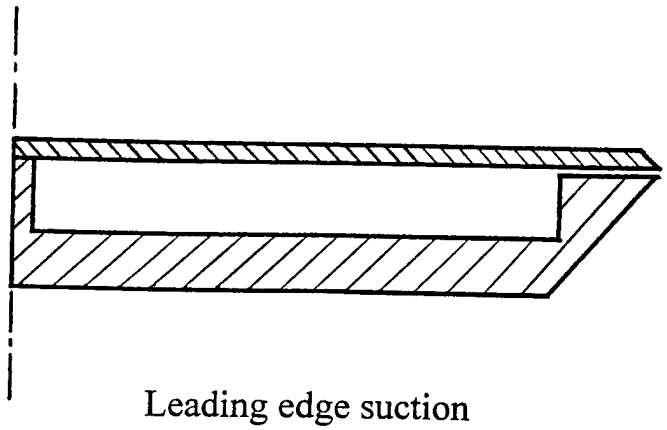

Leading edge suction

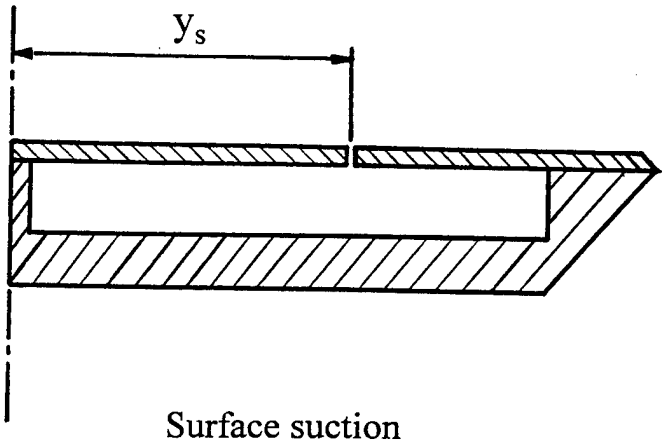

Surface suction

Figure 1: Schematic of leading-edge suction and surface suction.

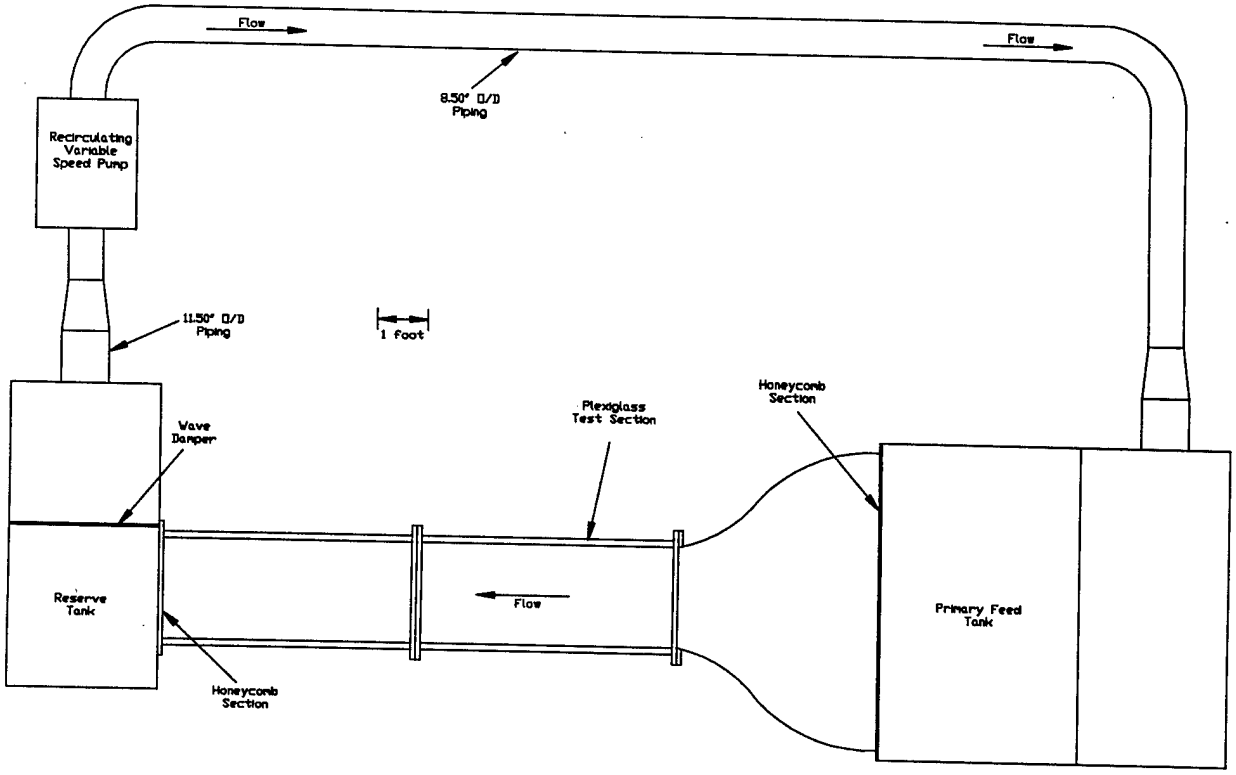

Figure 2: Schematic of water channel.

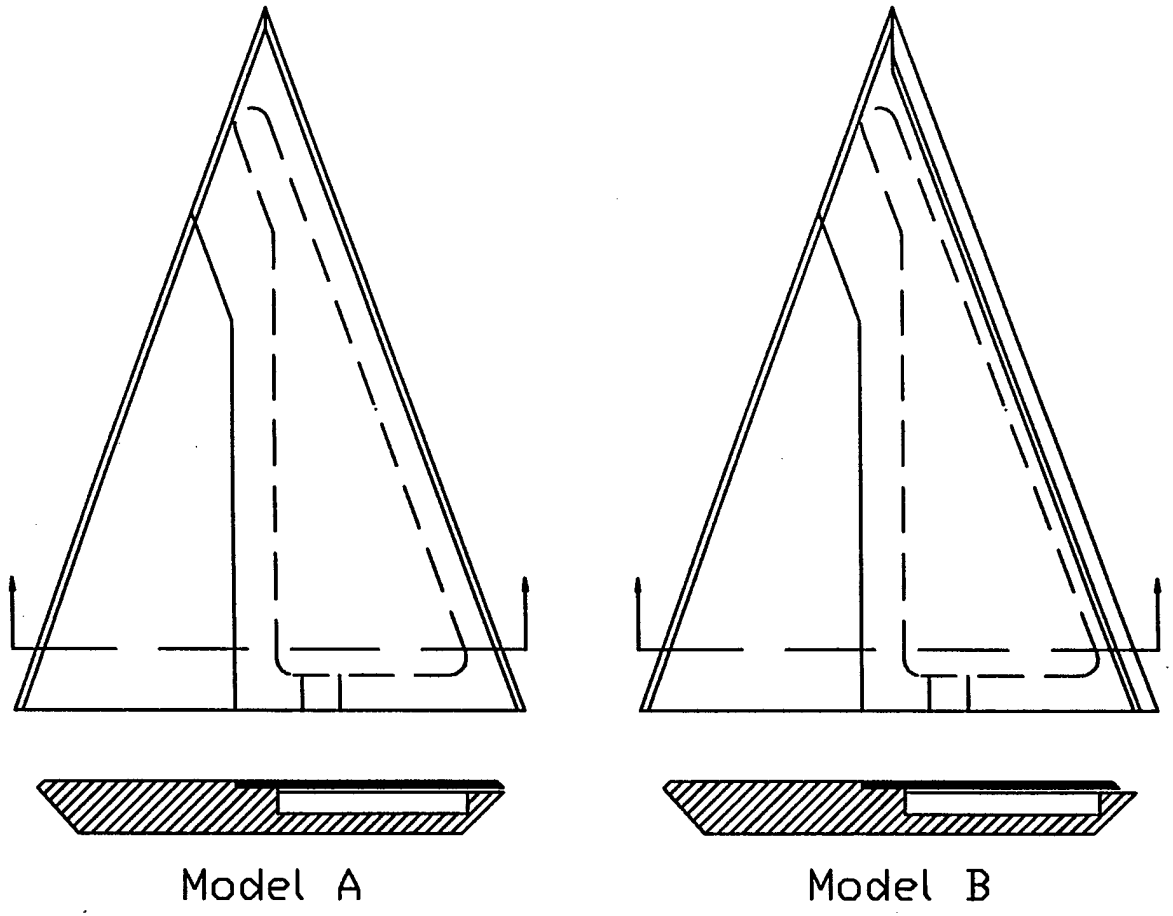

Figure 3: Model delta wings for Λ=70°.

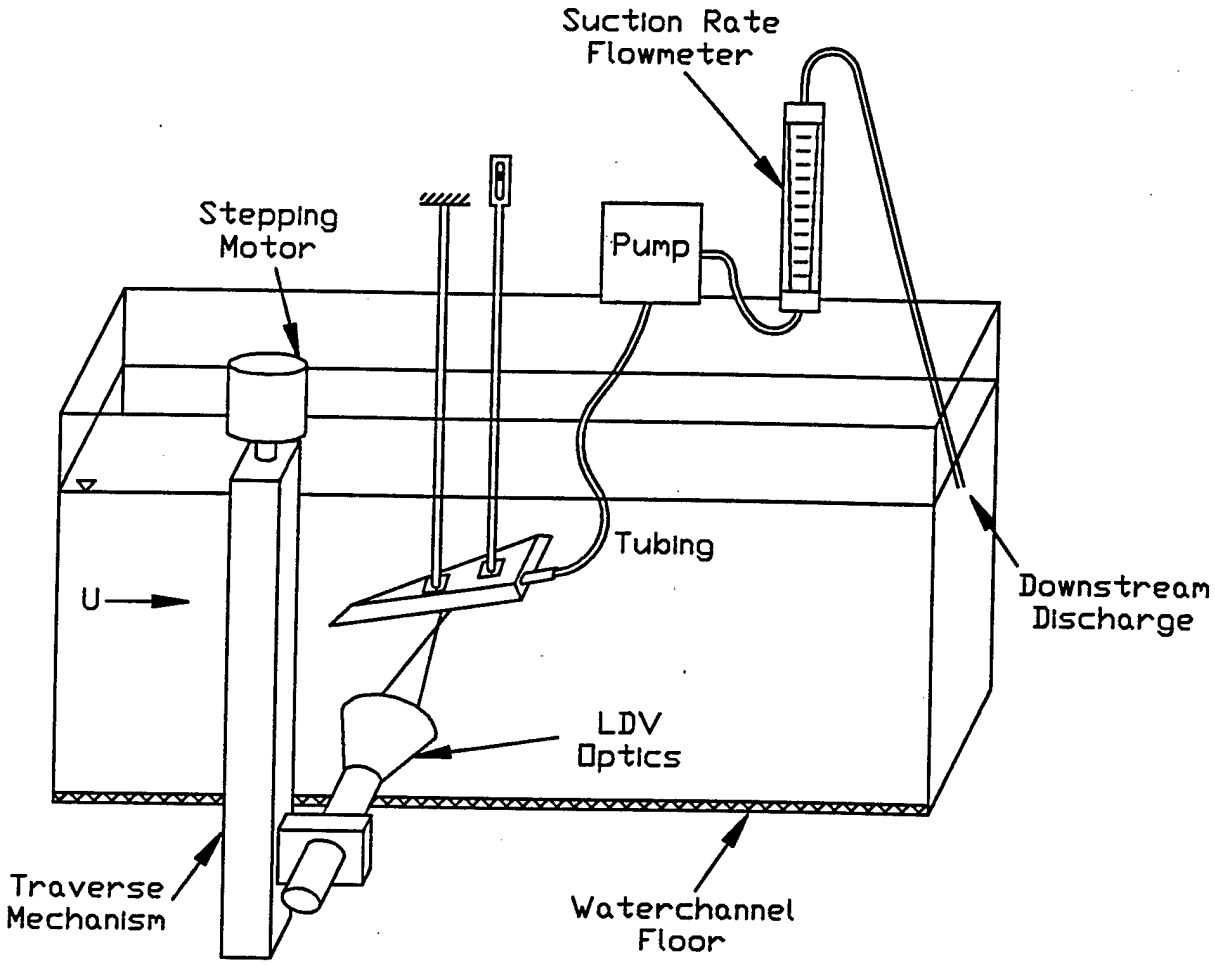

Figure 4: Schematic of suction system.

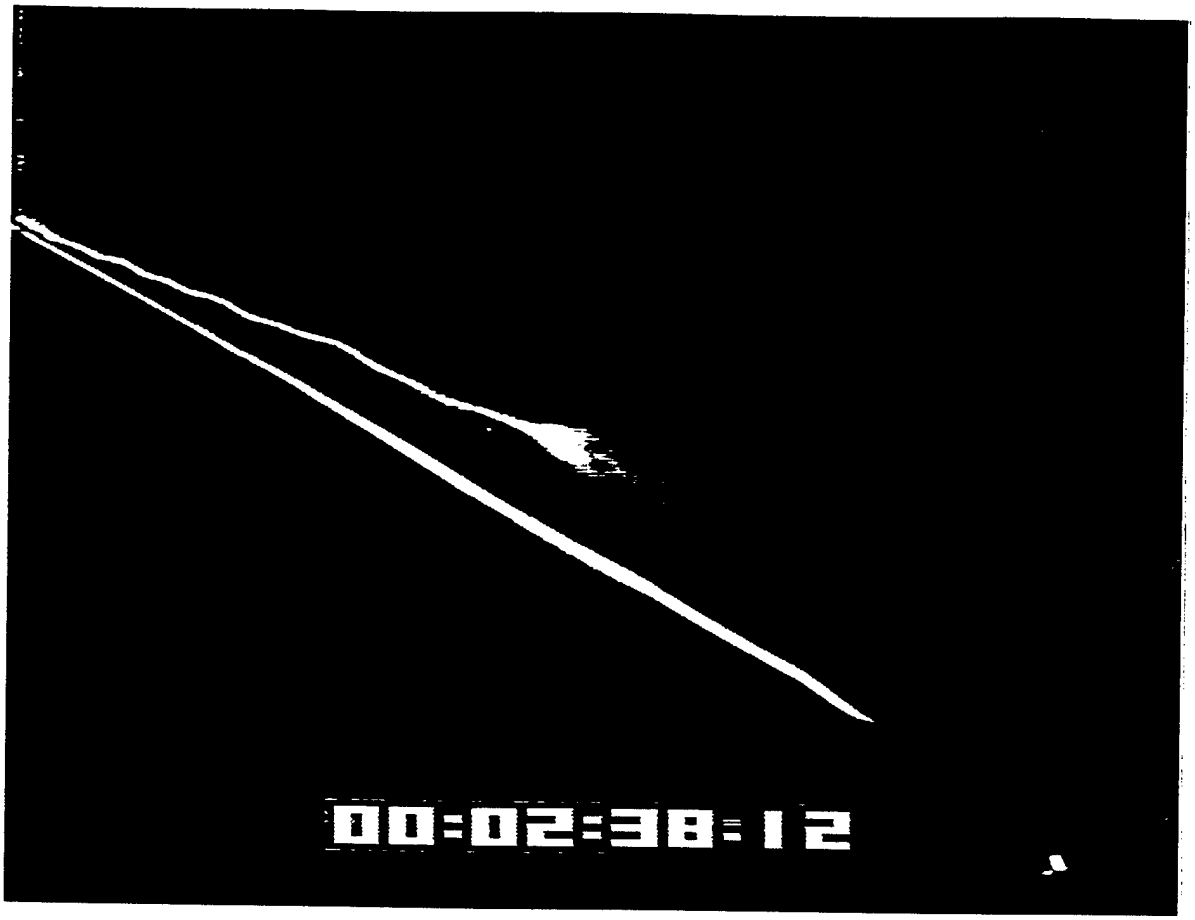

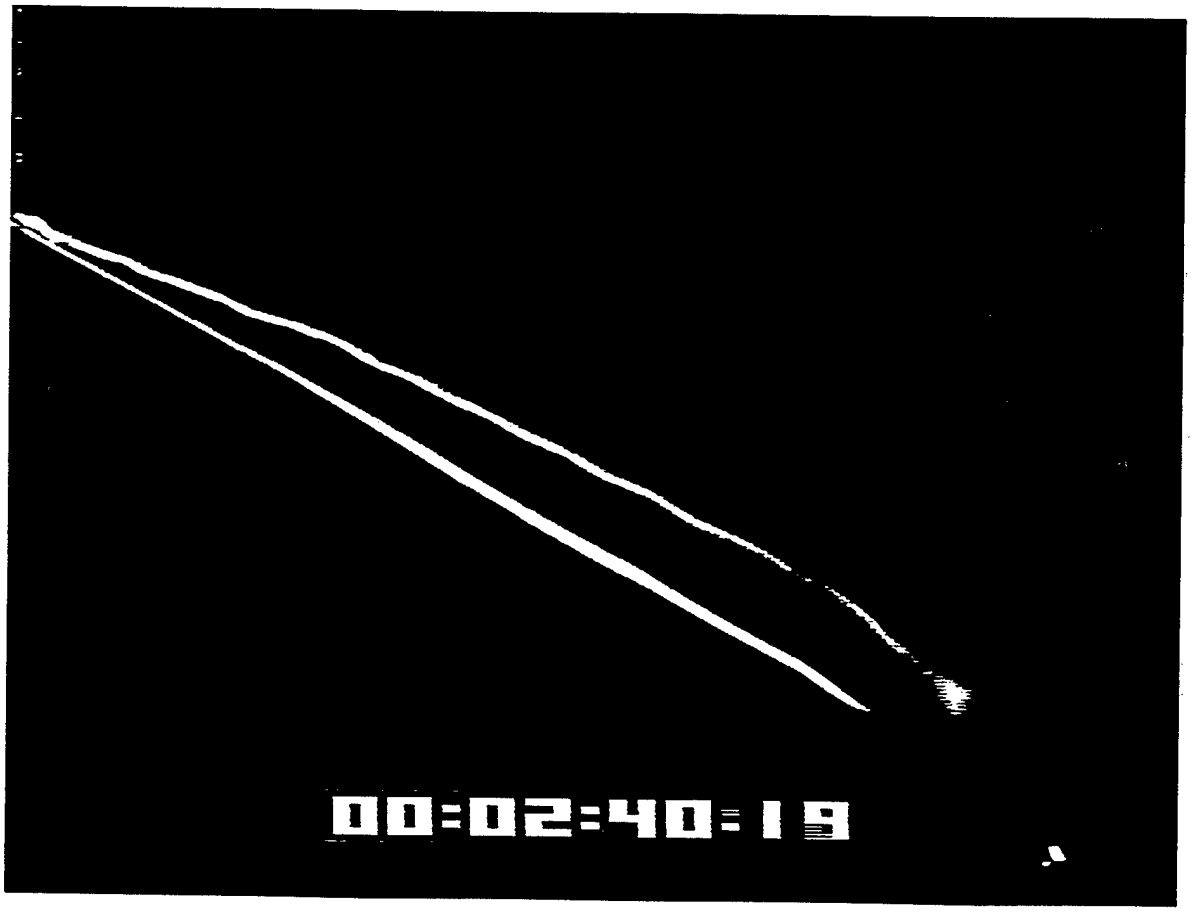

Figure 5: Flow visualization of vortex breakdown without suction (top) and with suction (bottom), $y_s/s=0.7$, $C_\mu=0.72$, $\alpha=25°$, Re=14,000.

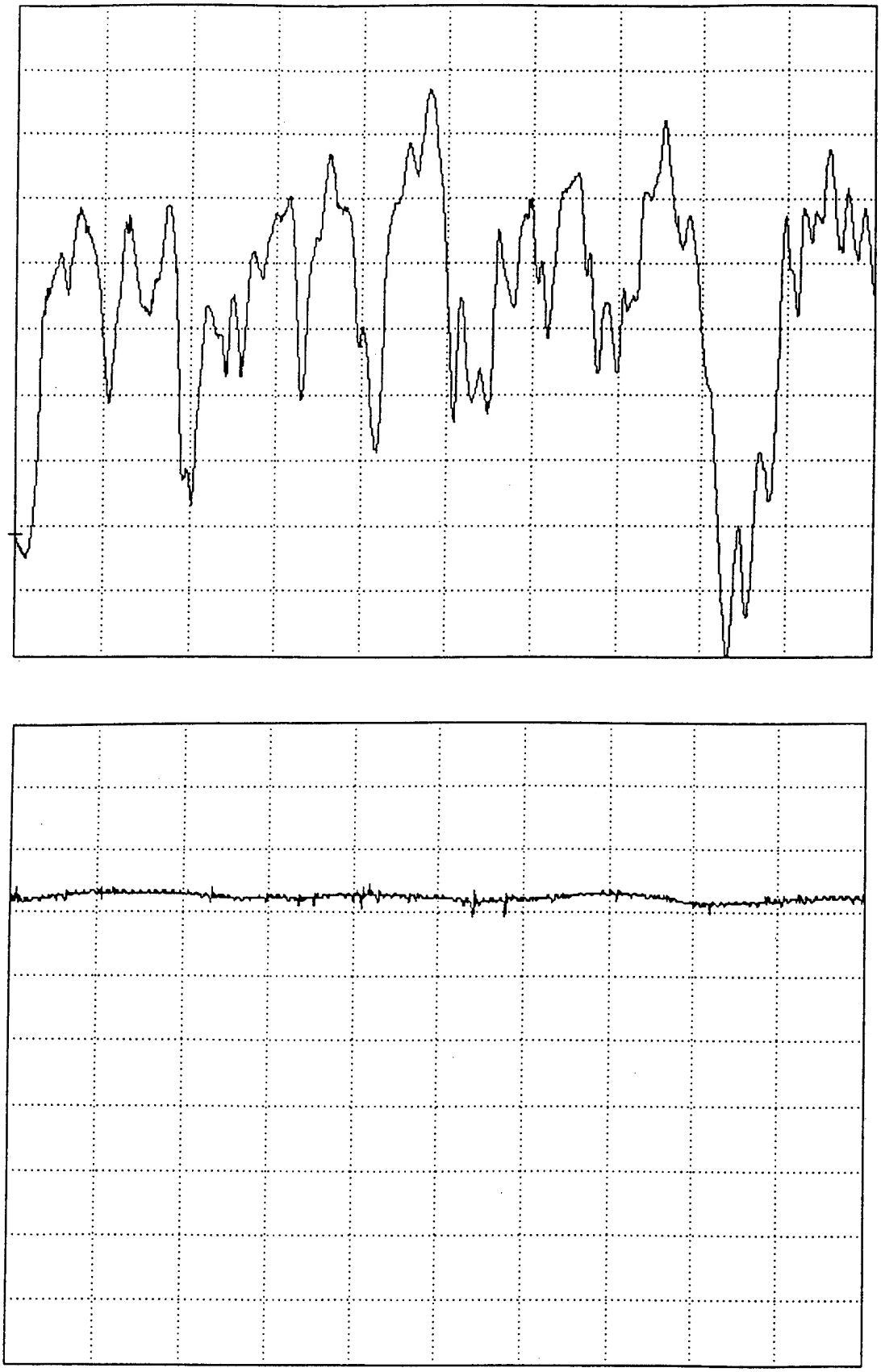

Figure 6: Hot-wire signals at (x/c=0.8, y/s=0.3, z/s=0.22) without suction (top) and with suction (bottom), y_s/s=0.7, C_μ=0.72, α=25°, Re=35,000.

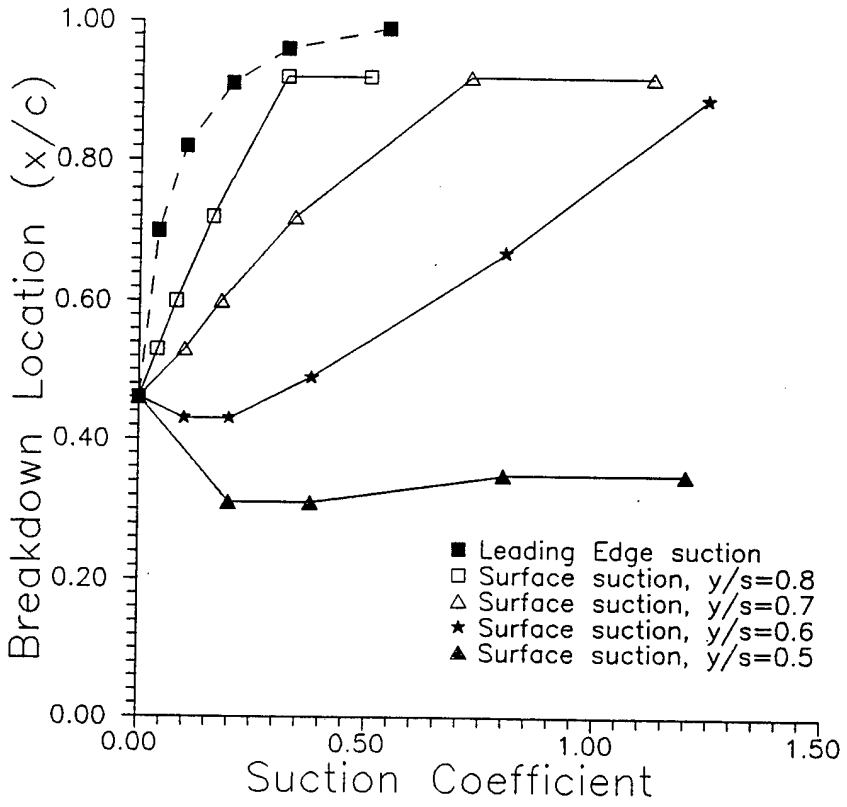

Figure 7: Variation of breakdown location as a function of suction coefficient.

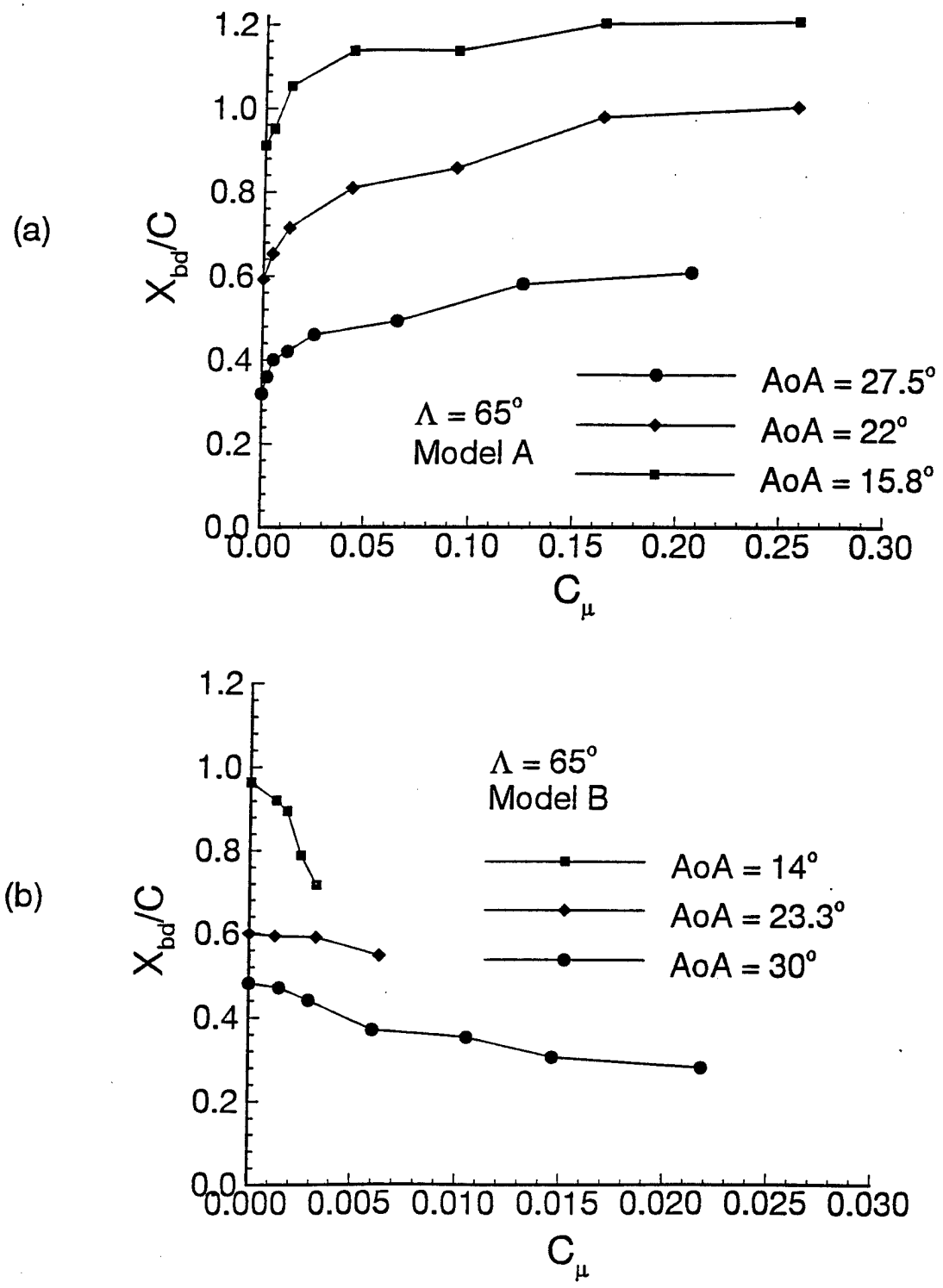

Figure 8: Variation of breakdown location with suction coefficient for (a) Model A, (b) Model B, Λ=65°.

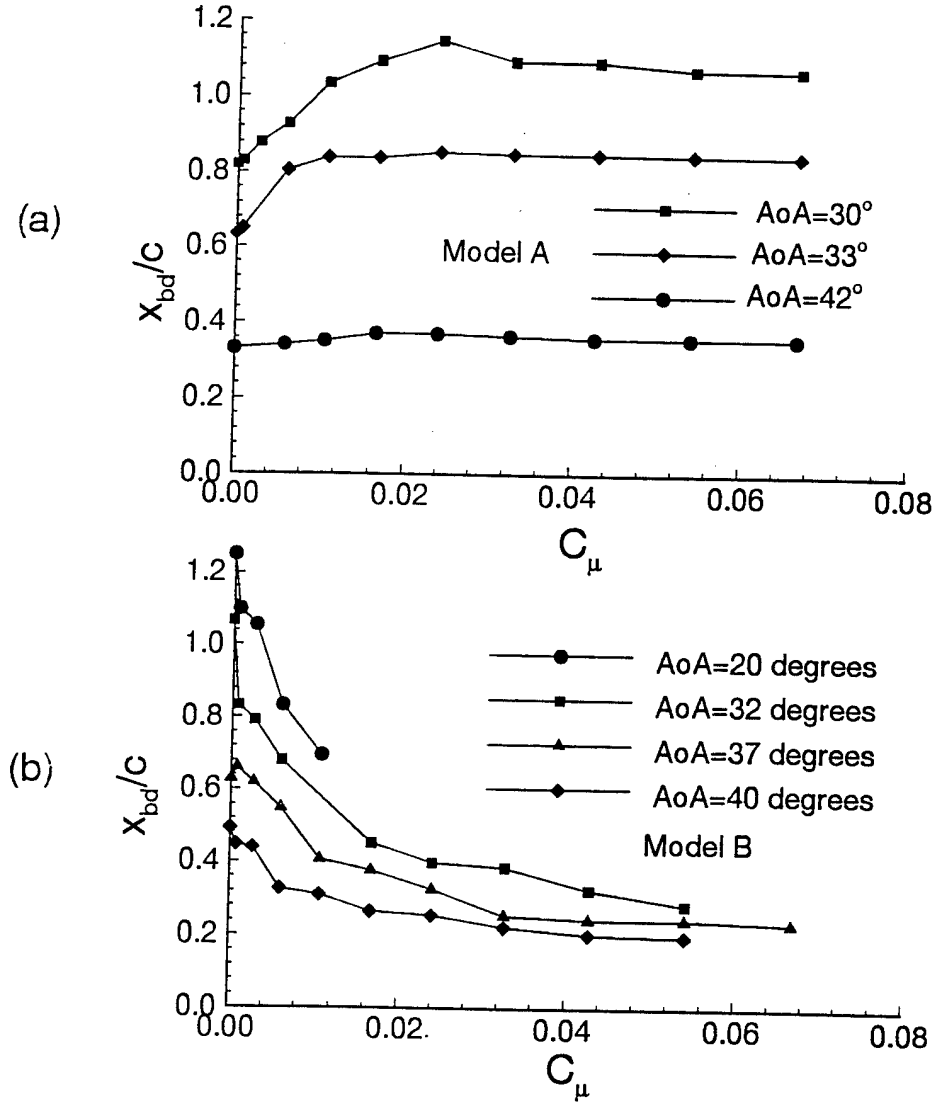

Figure 9: Variation of breakdown location with suction coefficient for Models A and B, Λ=70°.

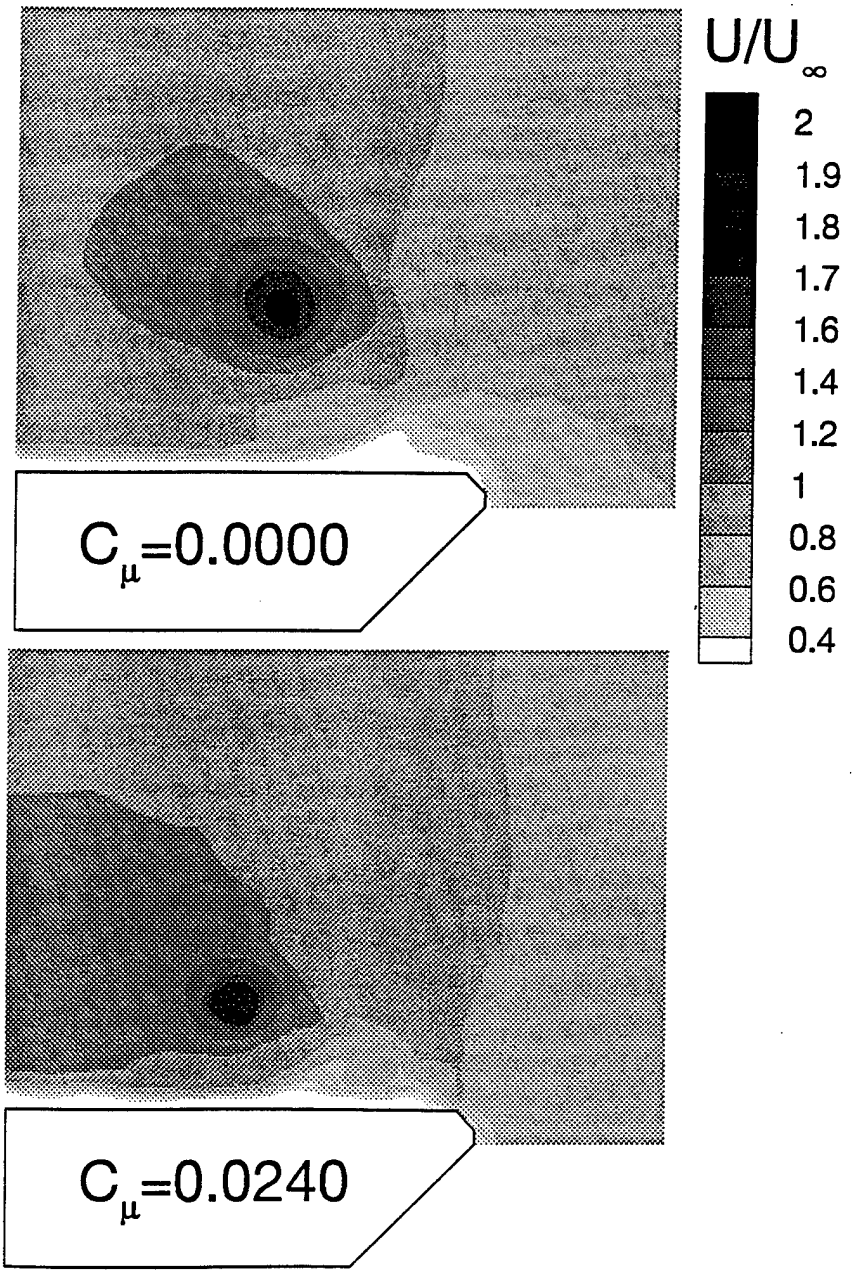

Figure 10: Contours of normalized time-averaged axial velocity for C_μ=0 and C_μ=0.024, Model A, Λ=70°, α=30°, x/c=0.6.

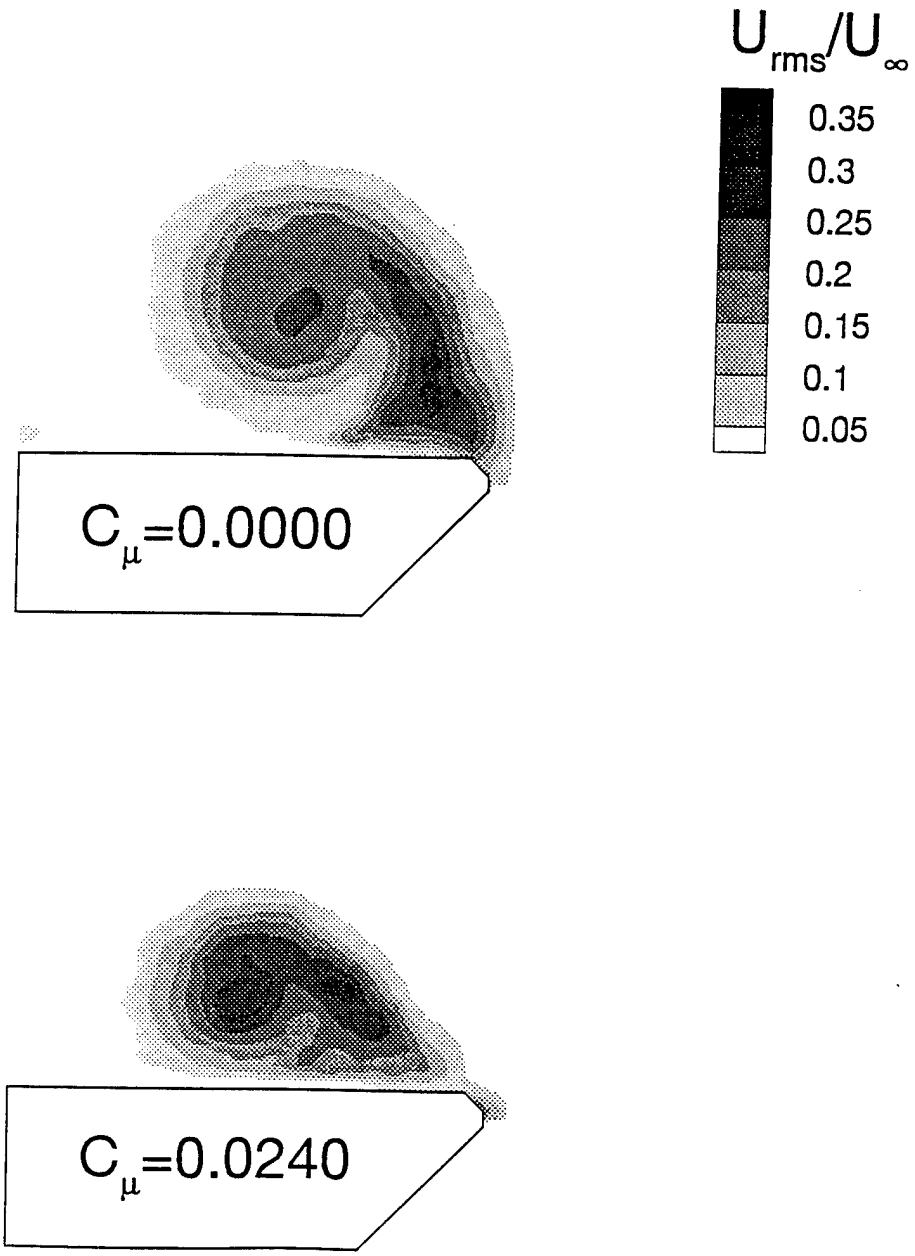

Figure 11:Contours of normalized rms axial velocity C_{μ}=0 and C_{μ}=0.024, Model A, Λ=70°, α=30°, x/c=0.6.

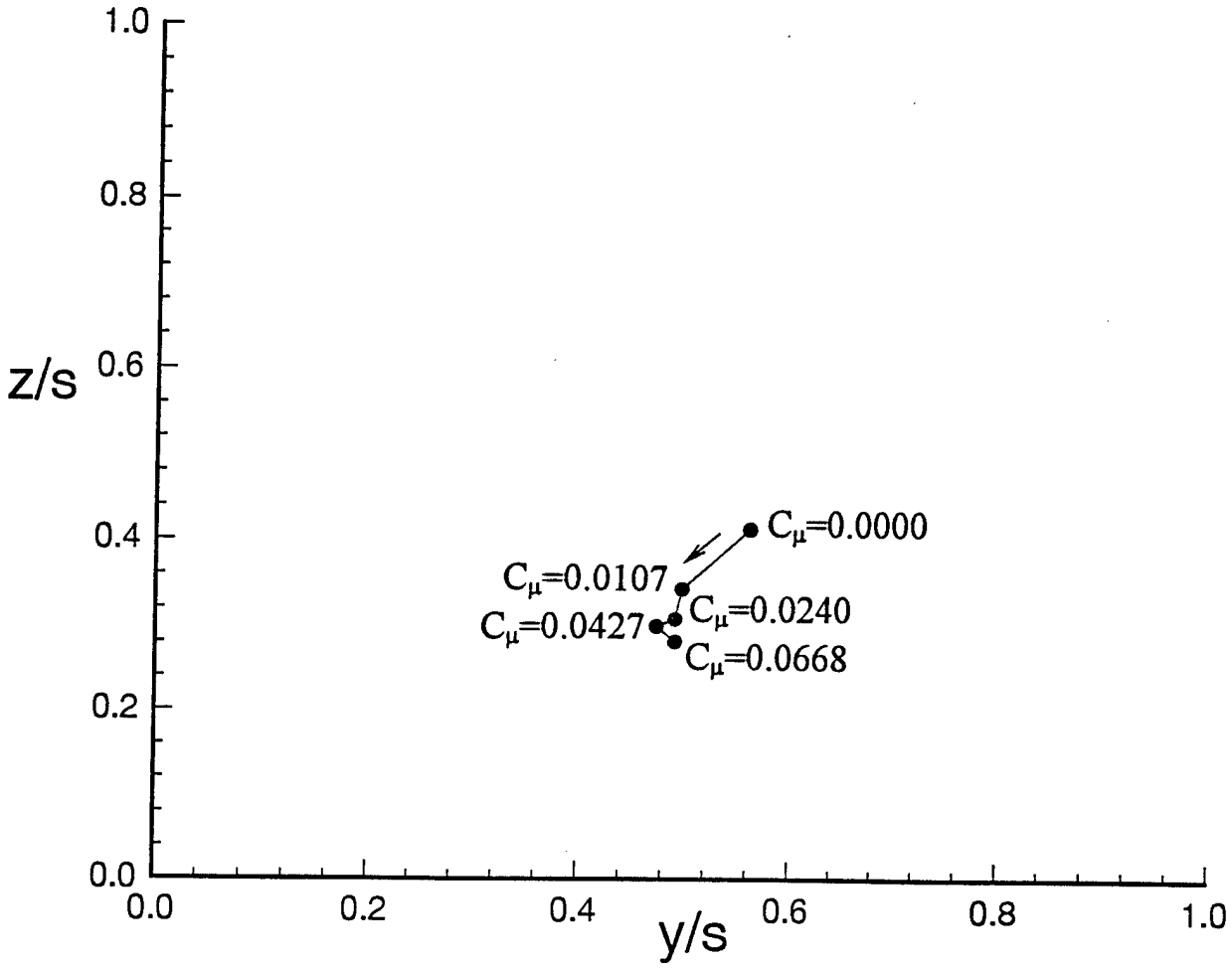

Figure 12: Variation of location of vortex core, Model A, Λ=70°, α=30°, x/c=0.6.

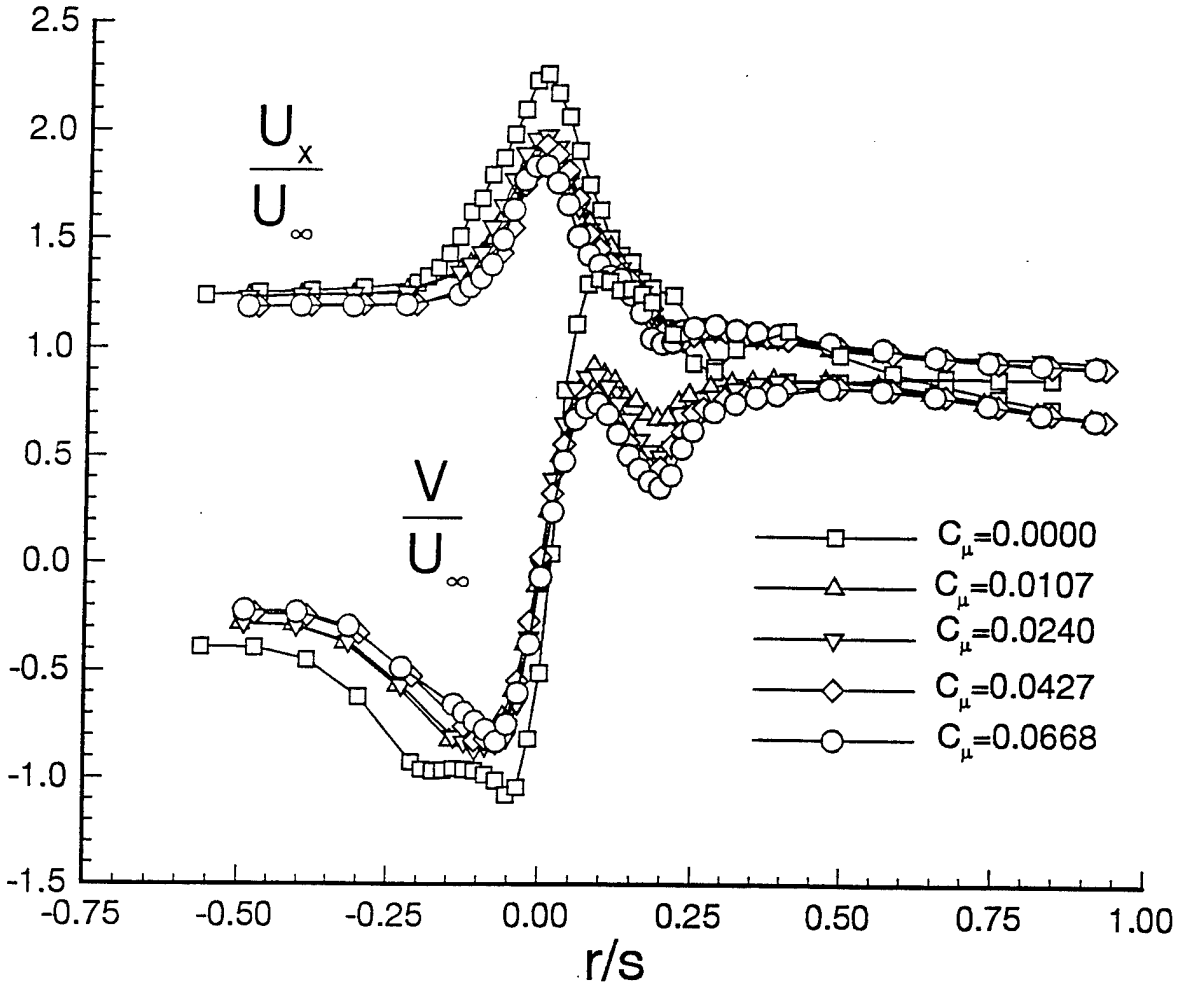

Figure 13: Variation of axial and swirl velocity across the core, Model A, Λ=70°, α=30°, x/c=0.6.

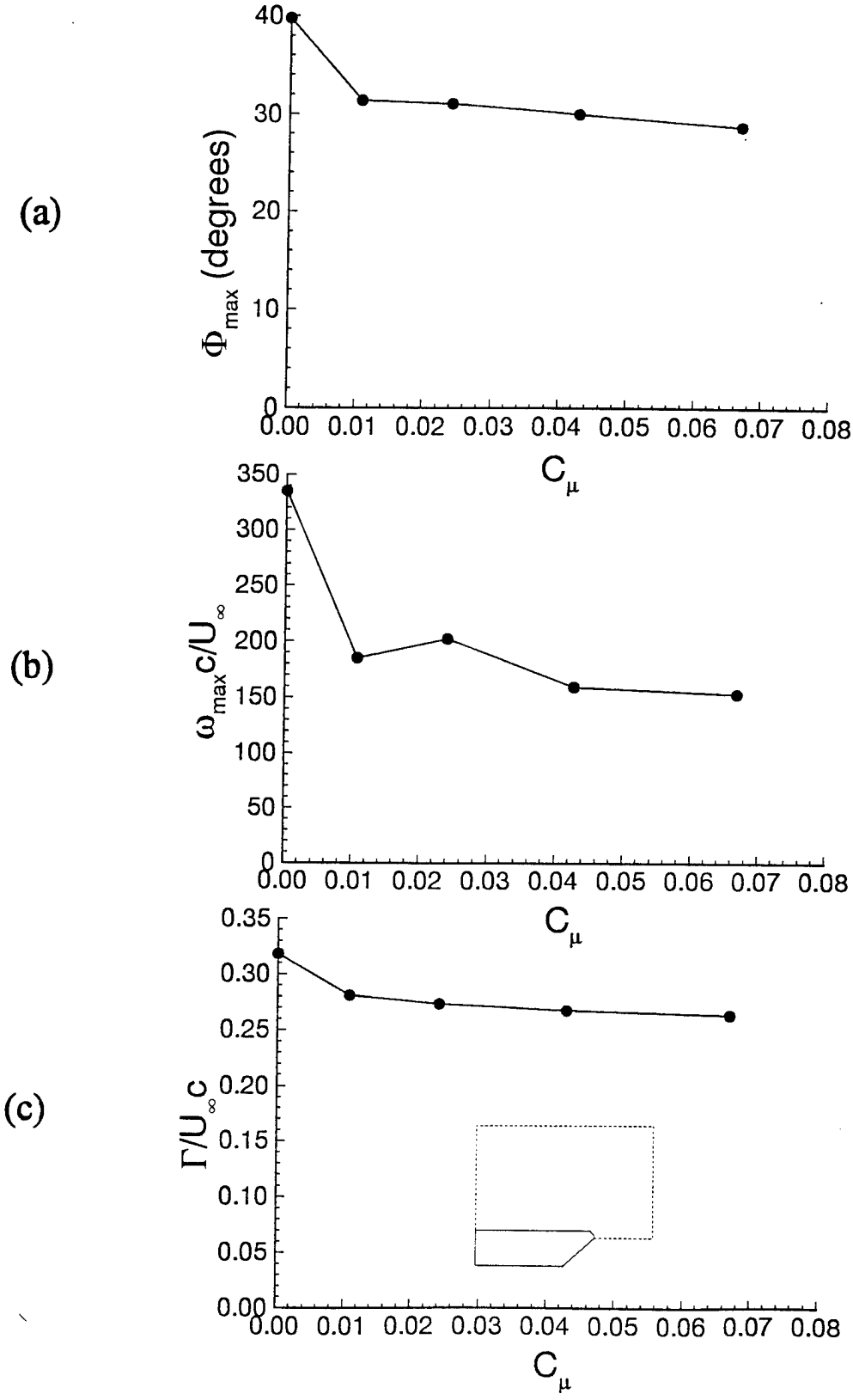

Figure 14: Variation of (a) maximum swirl angle (b) maximum axial vorticity (c) circulation with suction coefficient, Model A, Λ=70°, α=30°, x/c=0.6.

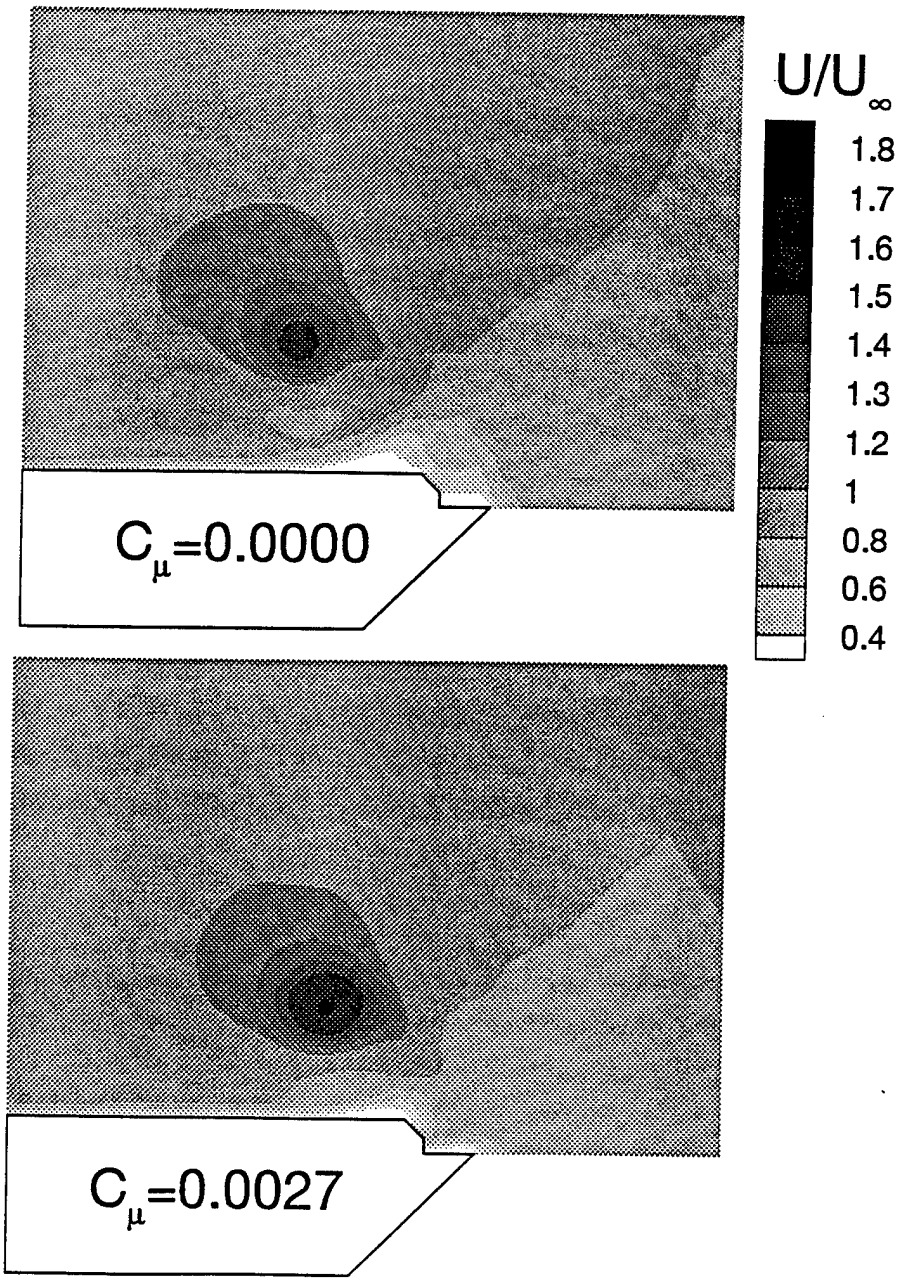

Figure 15: Contours of normalized time-averaged axial velocity for C_μ=0 and C_μ=0.0027, Model B, Λ=70°, α=20°, x/c=0.6.

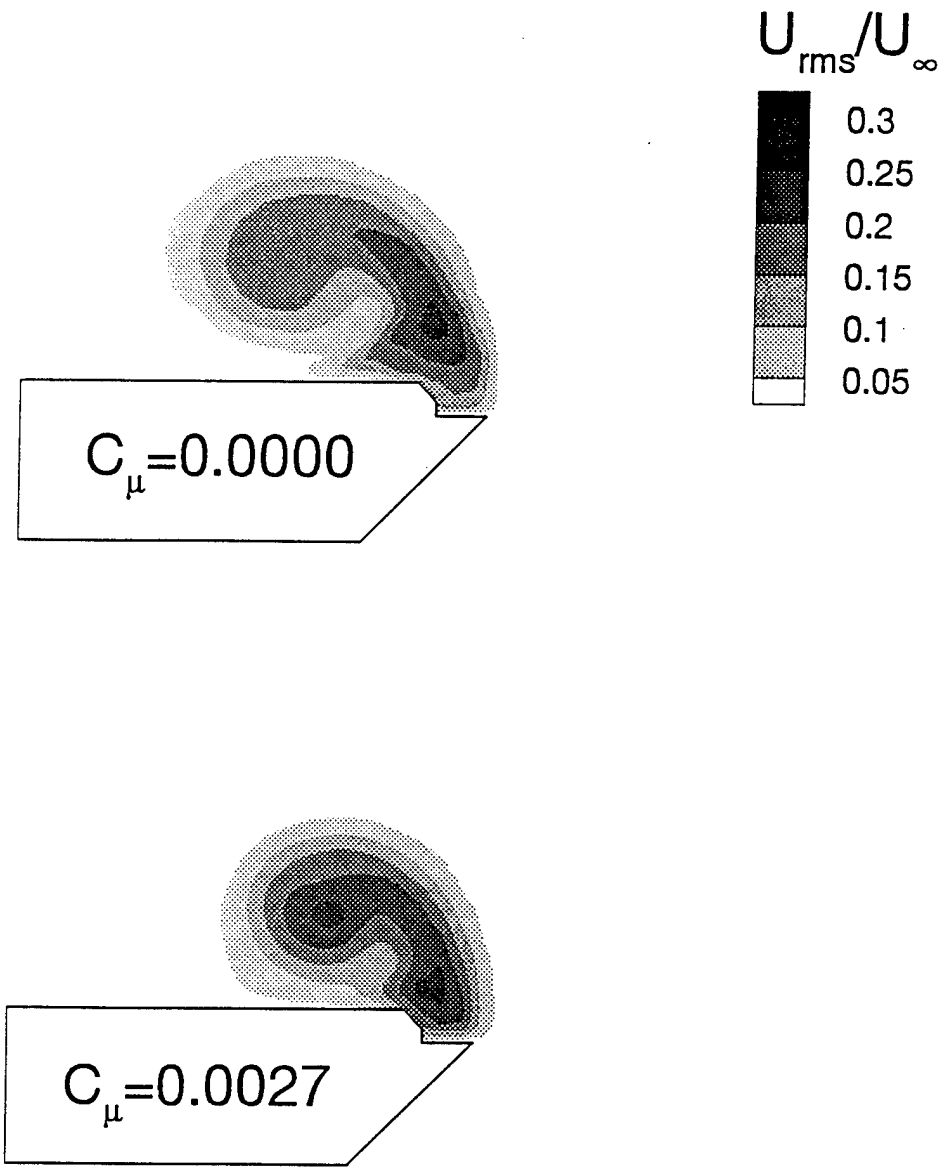

Figure 16: Contours of normalized rms axial velocity C_{μ}=0 and C_{μ}=0.0027, Model B, Λ=70°, α=20°, x/c=0.6.

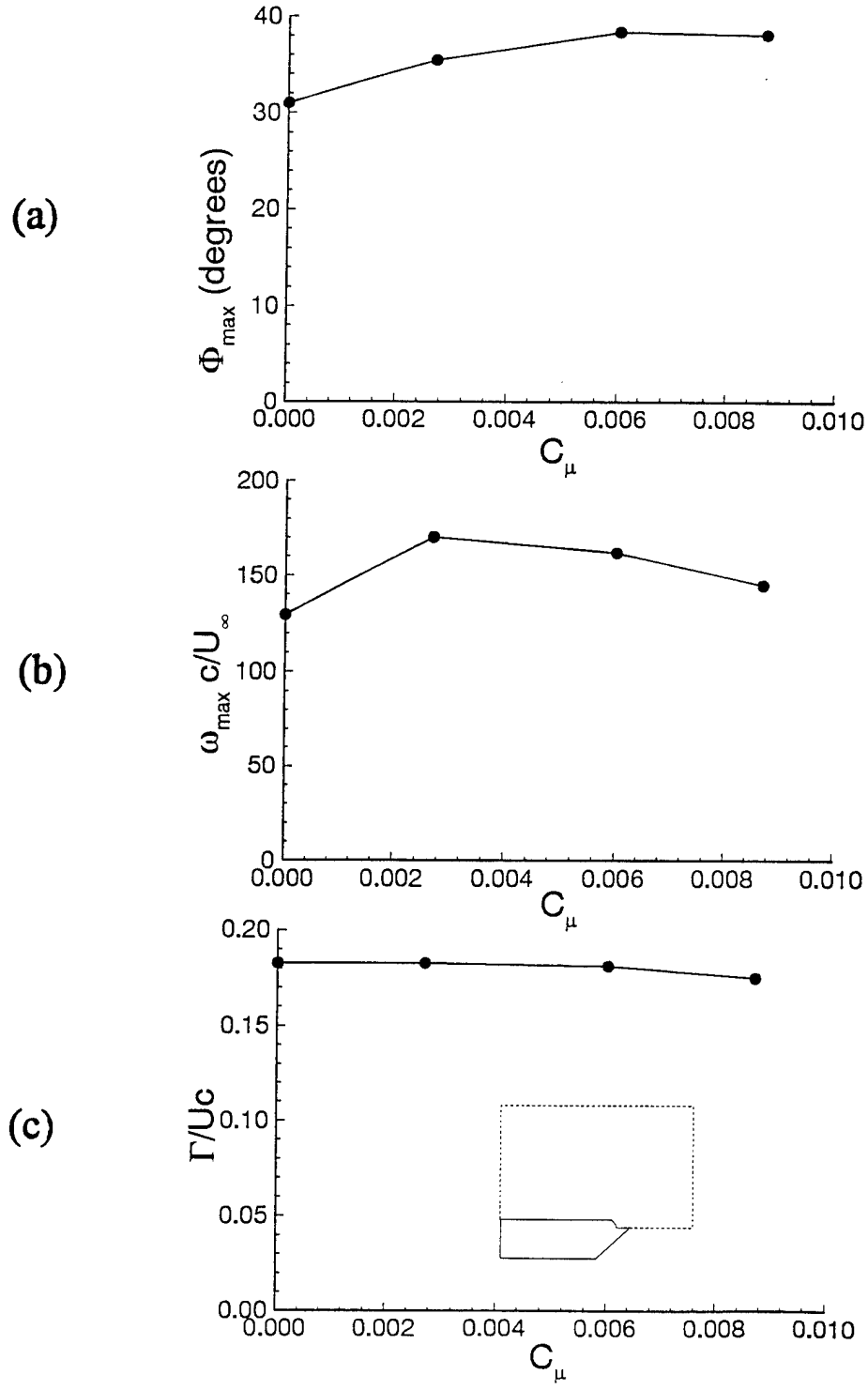

Figure 17: Variation of (a) maximum swirl angle (b) maximum axial vorticity (c) circulation with suction coefficient, Model B, Λ=70°, α=20°, x/c=0.6.

Vol. 33, No. 5, September–October 1996

Effect of Shear-Layer Control on Leading-Edge Vortices

S. McCormick* and I. Gursul†
University of Cincinnati, Cincinnati, Ohio 45221-0072

The effect of shear-layer control on leading-edge vortices over delta wings with sharp leading edges was investigated. By using suction near the separation point, the direction of the shear layer, and the location of the main vortex as well as its structure could be modified. The maximum swirl angle in the core and overall circulation decreased with suction. This caused the vortex breakdown location to move downstream. When the suction slot was located slightly inboard, the swirl angle was found to increase, causing the breakdown location to move upstream. It is shown that extremely small amounts of leading-edge suction can modify the location of the vortex core and can thus be used to induce rolling moment.

Nomenclature

A_s = cross-sectional area of suction slot
C_μ = suction coefficient, $(V_s/U_\infty)^2(A_s/S)$
c = root chord
Re = Reynolds number
r = radial distance from vortex axis
S = surface area of the wing
s = local semispan
U = time-averaged axial velocity
U_∞ = freestream velocity
u_{rms} = rms axial velocity
V = time-averaged swirl velocity
V_s = suction velocity
x = chordwise distance from the apex of the wing
x_{bd} = chordwise location of vortex breakdown
y = spanwise distance from wing root
z = distance above wing surface
α = angle of attack
Γ = circulation
Λ = sweep angle
ϕ = swirl angle, $\tan^{-1}V/U$
ω = vorticity

Introduction

VORTEX breakdown phenomenon continues to be a challenging aspect of vortical flowfields. Since highly maneuverable aircraft are designed to operate at high angle of attack, vortex breakdown may move onto the wing and affect the stability of the aircraft. The unsteady characteristics[1,2] of the flowfield downstream of breakdown are very important for stability and buffeting considerations.

Since the vorticity of the leading-edge vortices originates from the separation point along the leading edge, shear-layer control can be used to influence the strength and structure of these vortices. Several efforts have been reported in this direction: blowing and suction in the tangential direction along a rounded leading-edge[3,4]; and use of leading-edge flaps.[5–9] The study of Wood et al.[3] showed that a rounded, as opposed to a sharp, leading edge can alter the location of separation from the leading edge by tangential blowing. It has been pointed out that this technique uses the Coanda jet effect to help the shear layer attach to the convex surface.[10] Therefore, the application of this technique requires thick rounded leading edges. Leading-edge flaps are also known to be capable of controlling the separated shear layer and the leading-edge vortices. Stationary as well as oscillating flaps have been studied with the control of vortex breakdown in mind.[9]

One of the objectives of this work is to study the possibility of shear-layer control over delta wings with sharp leading edges. In an attempt to control the development of a two-dimensional shear layer, Leu and Ho[11] applied suction at the trailing edge of a splitter plate. It was shown that the free shear layer is sensitive to the modifications at the origin. The shear layer could be turned to a direction that is about 45 deg from the streamwise direction. This type of flow vectoring was also studied by direct numerical simulations.[12] Gad-el-Hak and Blackwelder[13] applied periodic perturbations of injection and suction along the leading edge of a delta wing. They found maximum changes in the evolution of the shear layer when the frequency of perturbations is the subharmonic of the frequency of Kelvin–Helmholtz instability. However, no results were reported regarding the structure of the main vortex and the effect on vortex breakdown. In this work, motivated by previous results, a similar shear-layer control technique is explored over a delta wing with sharp leading edges. Suction is applied along the leading edge of a delta wing through a slot, and it is shown that the separated shear layer can be effectively manipulated. This, in turn, causes large modifications in the structure of the leading-edge vortices. At large angle of attack, vortex breakdown can be controlled as well. It is shown that application of the leading-edge suction technique does not require thick rounded leading edges. Control of vortices can be achieved without the use of the Coanda jet effect.

Experimental Facility

The majority of the experiments were carried out in a water channel with a cross-sectional area of 610 by 610 mm. The turbulence intensity in the water channel is 0.6%. Experiments were carried out for two different types of model delta wings (called models A and B). In the water channel experiments, delta wings with sweep angles $\Lambda = 65$ and 70 deg were tested. In Fig. 1, the model delta wings are shown for $\Lambda = 70$ deg. Model A is the basic delta wing, whereas model B has a shorter upper plate that is parallel to the leading edge. At the trailing edge of the wing, the span of the upper plate is 93.4% of the semispan. Since the shear layer turns inboard over the upper surface of the wing for the conventional wings, it was decided to study other configurations for which the upper plate is shorter and is not expected to interfere with the curved shear layer. A third configuration that is similar to model B was also

Presented as Paper 96-0541 at the AIAA 34th Aerospace Sciences Meeting and Exhibit, Reno, NV, Jan. 15–18, 1996; received Jan. 28, 1996; revision received May 22, 1996; accepted for publication May 22, 1996.

*Graduate Student.
†Assistant Professor, Department of Mechanical, Industrial and Nuclear Engineering. Member AIAA.

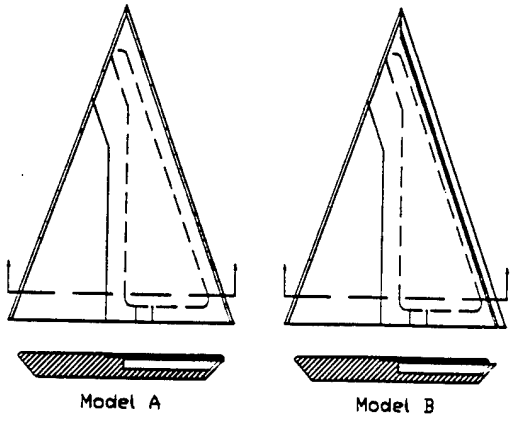

Fig. 1 Model delta wings for Λ = 70 deg.

tested. The span of the upper plate in this model varied linearly with the streamwise distance. The results are very similar to those for model B.[14] The leading edges were beveled at 45 deg on the windward side. The height of the suction slot is 1.8 mm. The chord lengths are c = 254 mm for Λ = 70 deg and c = 203 mm for Λ = 65 deg. The maximum blockage ratio was 5.6%. The Reynolds number based on chord length was in the range of $Re = 4 \times 10^4$ to 5×10^4. The freestream velocity was U_∞ = 20 cm/s, and no free surface effects were observed even at the highest angle of attack (α = 42 deg). The body of the models was made of Plexiglas® and the upper plates were made of stainless steel.

Flow visualization of vortex breakdown was done by injecting fluid with food coloring dye near the apex of the models. The flow visualization was videotaped for further analysis. The velocity was measured with a single component laser Doppler velocimetry (LDV) system. The measurement volume was 0.1 mm in diameter and 0.81 mm in length. For axial velocity measurements, the velocity component parallel to the wing surface was measured. Since the measurements were taken parallel to the trailing edge (which is not perpendicular to the vortex axis), the velocity component approximately corresponds to the axial velocity. Also, measurements of the velocity component normal to the wing surface were taken in the plane containing the vortex core axis. As the measurements were taken along a traverse line parallel to the wing surface, the normal velocity approximately corresponds to the swirl velocity across the vortex core. The traversing system used a minimum step of 1 mm, which translated to a grid resolution of $\Delta y/s = \Delta z/s = 0.0175$ at $x/c = 0.6$. The measurement uncertainties for breakdown location and mean velocity were estimated as 0.4 and 1%, respectively.

Preliminary flow visualization experiments were carried out in a wind tunnel with a cross-sectional area of 305 by 305 mm. The turbulence intensity in the wind tunnel was 0.25%. The model delta wings had a sweep angle of Λ = 65 deg. The maximum blockage ratio was 3%. The Reynolds number was around $Re = 1.2 \times 10^4$. Smoke injected near the apex helped to visualize the vortex core and provided information on vortex breakdown location.

The suction flow was generated by a pump or fan (for water channel and wind-tunnel experiments) located outside the test section. The volume flow rate for suction was measured by a rotameter-type flow meter. Further information regarding the experimental setup and instrumentation can be found in Ref. 14.

Results

From the wind-tunnel experiments for Λ = 65 deg, the variation of breakdown location with suction coefficient is shown in Fig. 2 for models A and B. The fundamental difference in the response of models A and B is that the breakdown location moves downstream for model A, whereas the breakdown location moves upstream for model B. For model A, vortex breakdown location could be delayed up to 40% of the chord length. When compared with the results by Gu et al.,[4] this maximum improvement is nearly the same. Also, for model A, the breakdown location reaches a nearly constant level at larger values of the suction coefficient. Although suction causes the vortex core to get closer to wing surface for both models, the location of the vortex core changes slightly with the suction coefficient for model A, whereas there is a large change of core location with small amounts of suction coefficient for model B.[14] In fact, similar amounts of change in the core location can be obtained with suction coefficients that are one order of magnitude smaller for model B than for model A.

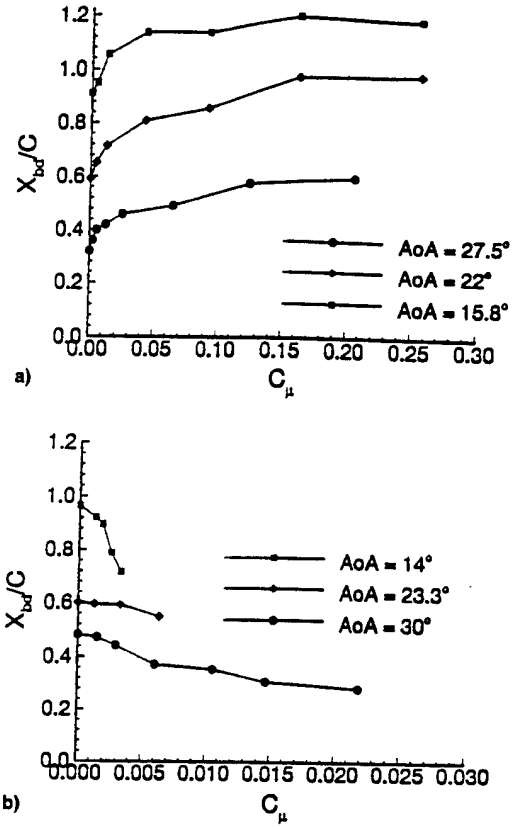

Fig. 2 Variation of breakdown location with suction coefficient for models a) A and b) B, Λ = 65 deg.

From the water channel experiments for Λ = 70 deg, the variation of breakdown location with suction coefficient is shown in Fig. 3 for models A and B. The results are qualitatively similar to those presented in Fig. 2. For model A, the effect of suction on breakdown is generally positive, except at very large angles of attack where suction does not make much difference. For α = 30 deg, the breakdown location reaches a maximum around C_μ = 0.024, after which it becomes nearly constant. Detailed LDV measurements were carried out for α = 30 deg.

The constant contours of the normalized time-averaged axial velocity for x/c = 0.6 (upstream of the breakdown location) are compared in Fig. 4 for C_μ = 0 and 0.024 at which the breakdown location is at maximum downstream location. It is clear that the vortex core moves inboard and closer to the wing surface. There is also a slight decrease in the maximum axial velocity with suction. The constant contours of the normalized rms axial velocity are compared in Fig. 5 for C_μ = 0 and 0.024. The shape of the rms velocity contours is a good indicator of the shear layer and main vortex. (This was also shown for vortical flows over a body of revolution at incidence.[15] The high rms velocity fluctuations indicated the location of the vortex cores. The rms velocity contours were found to be repre-

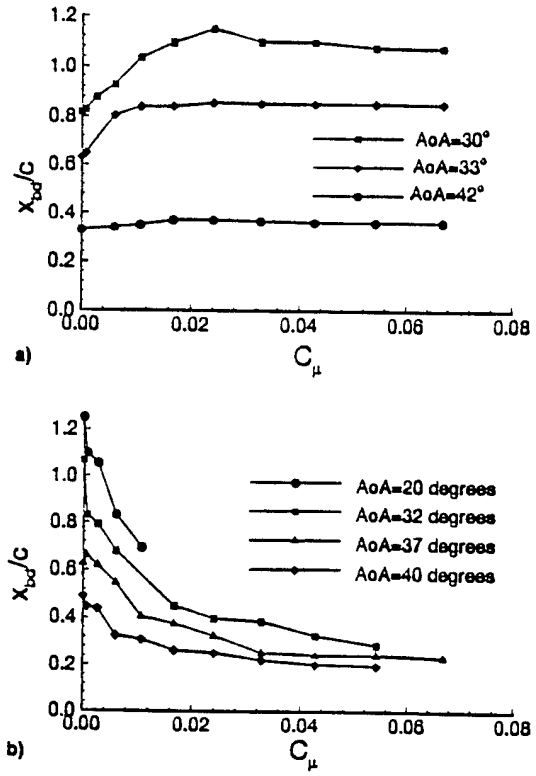

Fig. 3 Variation of breakdown location with suction coefficient for models a) A and b) B, Λ = 70 deg.

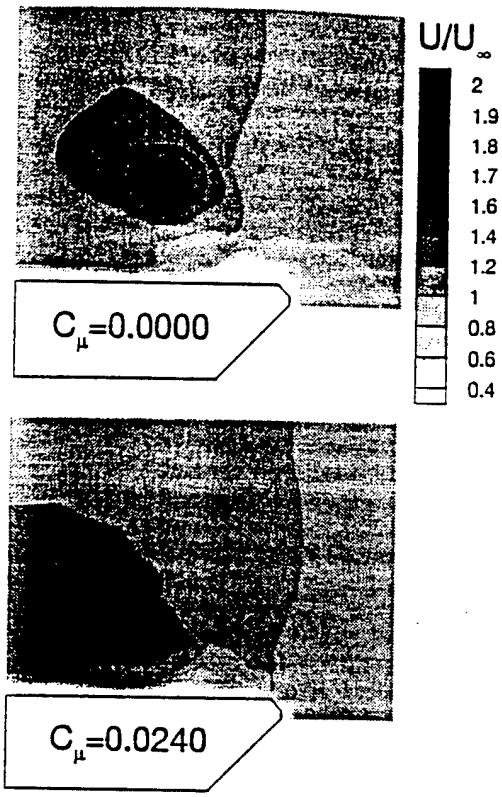

Fig. 4 Contours of normalized time-averaged axial velocity for C_μ = 0 and 0.024, model A, Λ = 70 deg, α = 30 deg, and x/c = 0.6.

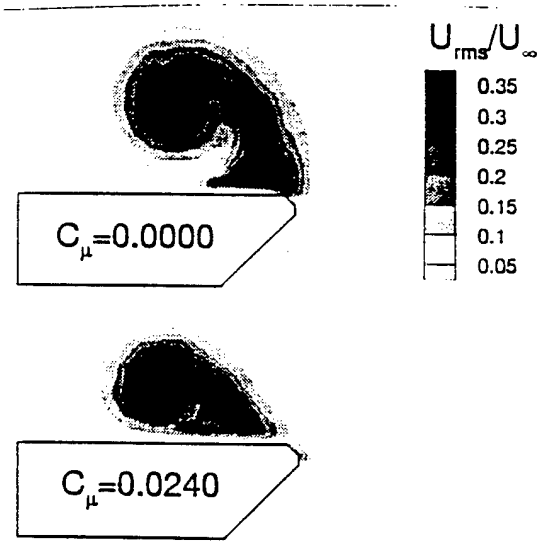

Fig. 5 Contours of normalized rms axial velocity C_μ = 0 and 0.024, model A, Λ = 70 deg, α = 30 deg, and x/c = 0.6.

sentative of the cross sections of the tip vortices.) In the present experiments, very large levels of rms velocity (up to 30% of the freestream velocity) in the shear layer and in the core of the leading-edge vortex were observed. It should be noted that this high rms velocity level is observed well upstream of the breakdown location. Other experiments in vortical flows (in the absence of breakdown) showed very high levels of rms velocity.[13-17] This is not very surprising if the dynamics of the shear layer is considered (i.e., development of coherent structures and pairing, etc.). Although a high level of rms velocity was reported in the vortex cores previously for large Reynolds numbers, the existence of high levels was not known for relatively low Reynolds numbers (based on the chord length) such as $Re = 5 \times 10^4$. It is clear from Fig. 5 that, with suction, the direction of the shear layer is changed. It is also evident that the vortex core moves inboard and toward the wing surface with suction.

Since suction was applied along one of the leading edges, its effect on the other vortex was investigated.[14] Time-averaged axial velocity and rms axial velocity contours (not shown here because of space limitations) revealed that there was no change in the structure of the other vortex. Therefore, suction can be used for independent control of leading-edge vortices, thus generating a net rolling moment. On the other hand, at very large angles of attack (α = 50 deg), the left and right vortical flows were shown to be strongly coupled.[3]

The constant contours of the normalized time-averaged axial velocity for x/c = 1.0 (downstream of the breakdown location in the absence of suction) are compared in Fig. 6 for C_μ = 0 and 0.024. Without suction, the flow retardation that is characteristic of breakdown is visible. The time-averaged axial velocity in the core drops to near zero values, and the size of the core increases greatly. With the suction, the axial velocity becomes jet-like and the core location gets closer to the wing. The constant contours of the normalized rms axial velocity are compared in Fig. 7 for C_μ = 0 and 0.024. With the suction, a decrease in the maximum rms velocity in the core is observed because of that is caused by the delay of the vortex breakdown. The change in the core location is also evident. Measurements of the swirl velocity across the core (not shown here) revealed that the size of the vortex core decreases and the axial vorticity increases with the suction, which is consistent with the changes associated with the movement of breakdown location downstream of the measurement plane.[14]

To quantify the effect of suction on upstream conditions (before breakdown) and on the parameters affecting breakdown, detailed measurements were taken at x/c = 0.6 for several values of the suction coefficient. The location of vortex core was found by locating the position of the maximum of the axial velocity distribution (at x/c = 0.6, upstream of breakdown location). Then, measurements of axial and swirl velocity components were taken across the vortex core. The variation of location of the vortex core is shown in Fig. 8. It is seen

that the vortex core moves slightly inboard and closer to the wing surface with increasing suction coefficient. However, with increasing suction coefficient, the changes in the core location become relatively small. The variation of axial and swirl velocities across the core is shown in Fig. 9. A decrease in the maximum axial velocity is observed with increasing suction. The maximum values of the swirl velocity also decrease with increasing suction. Slightly outboard of the core, a decrease and then a local maximum are observed (caused by shear layer), followed by a leveling of the swirl velocity. Based on the measured axial and swirl velocity components, the swirl angle ($\phi = \tan^{-1} V/U$) can be calculated as a function of the distance from the vortex axis. The variation of swirl angle with the distance from the vortex axis is given in detail in Ref. 14. The swirl angle is zero at the center of the vortex core and reaches a maximum at the edge of the subcore (the subcore being the region where most of the streamwise vorticity is confined). The variation of maximum swirl angle with the suction coefficient is shown in Fig. 10a. It is seen that there is a decrease in swirl angle with increasing suction coefficient, although the changes become more gradual at larger values of the suction coefficient. The axial vorticity distribution can also be calculated assuming rotational symmetry. In other words, the swirl velocity profile is sufficient to estimate the axial vorticity. The axial vorticity component is given by $\omega = \partial V/\partial r + V/r$. An example of the calculated vorticity distribution (by the forward differencing method) is given in Ref. 14. The maximum axial vorticity (which occurs at the vortex axis), is shown as a function of suction coefficient in Fig. 10b. A decrease in the maximum axial velocity with suction is observed. However, there is almost no change with further changes in the suction coefficient. In addition, the variation of circulation (obtained from the velocity measurements along the path shown in inset) is shown as a function of suction coefficient in Fig. 10c. The overall circulation decreases with increasing suction coefficient. Although this closed contour encloses the main vortex, secondary vortex, and shear layer, it is a reasonable indicator of the strength of the main vortex. Moreover, the circulation calculated this way can be interpreted as the rate at which vorticity is fed. In summary, it is shown that, for $\alpha = 30$ deg, suction delays the vortex breakdown for model A. This is because of a decrease in maximum swirl angle and circulation as well as in maximum axial vorticity. Further experiments for $\Lambda = 65$ deg also showed similar results.[14]

For model B, the flow visualization showed an opposite trend for the variation of breakdown location with suction (see Fig. 3). Therefore, it was decided to carry out detailed measurements for model B at $\alpha = 20$ deg. The constant contours

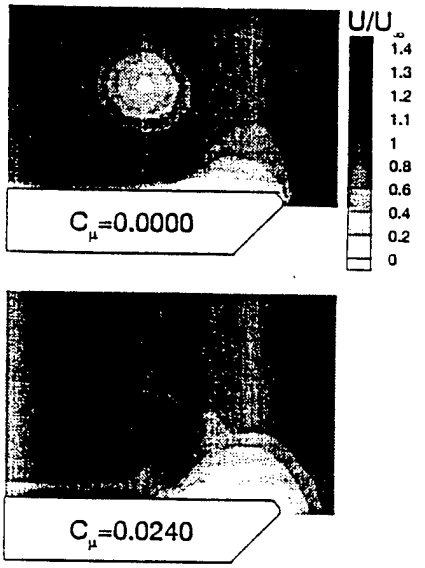

Fig. 6 Contours of normalized time-averaged axial velocity for $C_\mu = 0$ and 0.024, model A, $\Lambda = 70$ deg, $\alpha = 30$ deg, and $x/c = 1.0$.

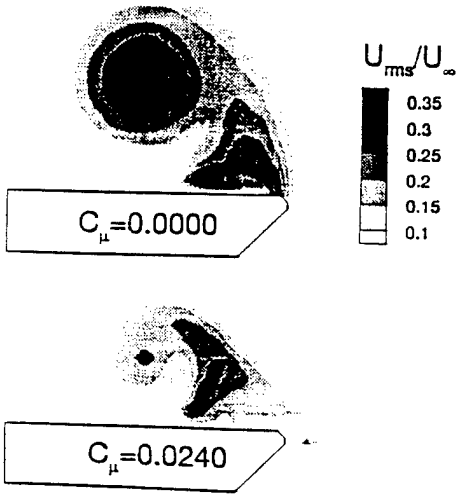

Fig. 7 Contours of normalized rms axial velocity $C_\mu = 0$ and 0.024, model A, $\Lambda = 70$ deg, $\alpha = 30$ deg, and $x/c = 1.0$.

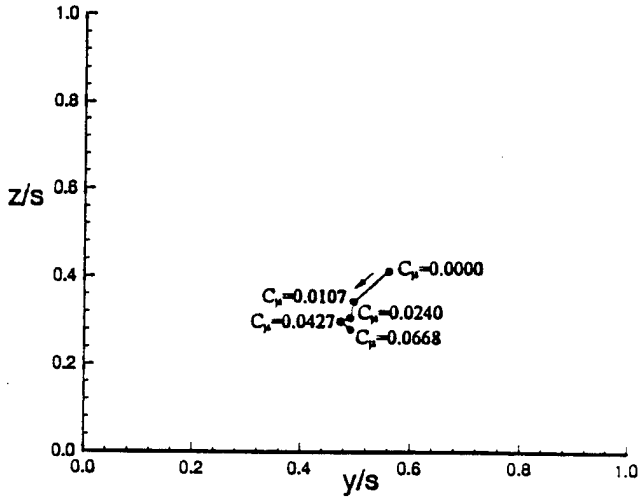

Fig. 8 Variation of location of vortex core, model A, $\Lambda = 70$ deg, $\alpha = 30$ deg, and $x/c = 0.6$.

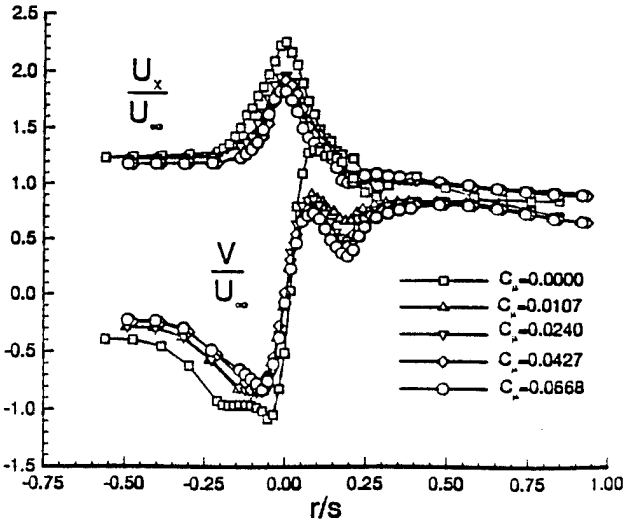

Fig. 9 Variation of axial and swirl velocity across the core, model A, $\Lambda = 70$ deg, $\alpha = 30$ deg, and $x/c = 0.6$.

of the normalized time-averaged axial velocity for $x/c = 0.6$ (upstream of the breakdown location) are compared in Fig. 11 for $C_\mu = 0$ and 0.0027. It is seen that an extremely small amount of suction (almost one-tenth of the amount used for model A) is sufficient to displace the vortex core. There is a slight increase in the maximum axial velocity. The constant contours of the normalized rms axial velocity shown in Fig. 12 indicate that the vortex core moves outboard and closer to the wing surface with suction. Higher levels of rms axial velocity are found in the core when suction is applied.

The location of vortex core was found from the axial velocity distributions (at $x/c = 0.6$, upstream of breakdown location). The variation of location of vortex core is shown in Fig. 13. It is seen that, initially, the vortex core moves outboard and closer to the wing surface with increasing suction coefficient. There is a small inboard displacement for the largest suction coefficient. The variation of axial and swirl velocities

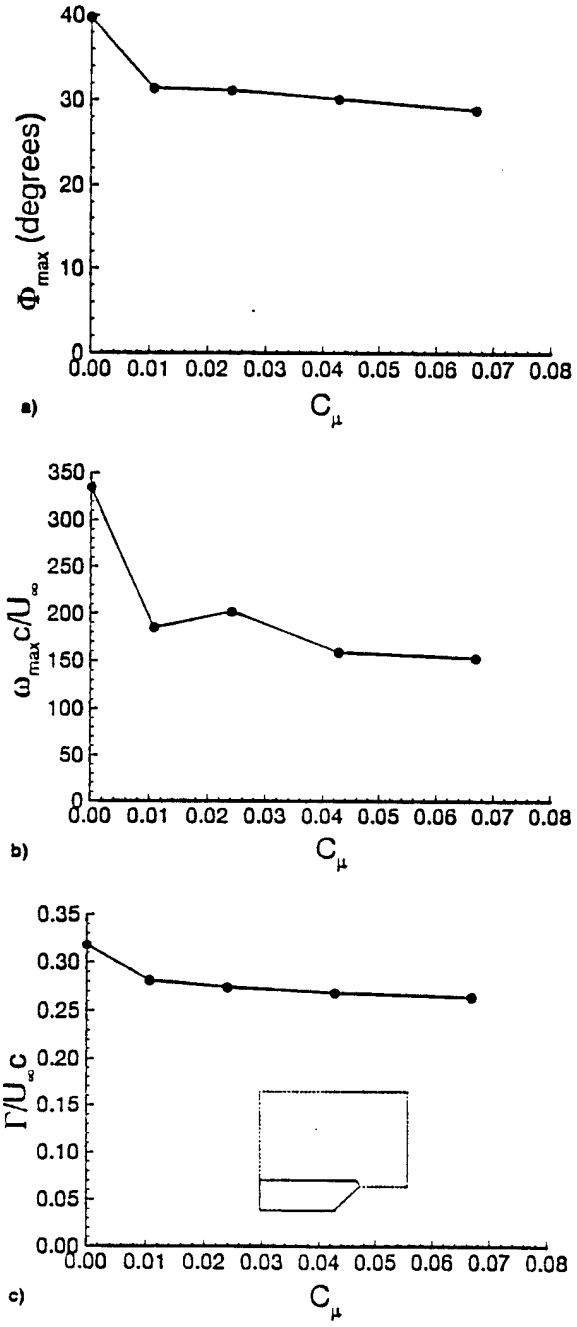

Fig. 10 Variation of a) maximum swirl angle, b) maximum axial vorticity, and c) circulation with suction coefficient, model A, Λ = 70 deg, α = 30 deg, and x/c = 0.6.

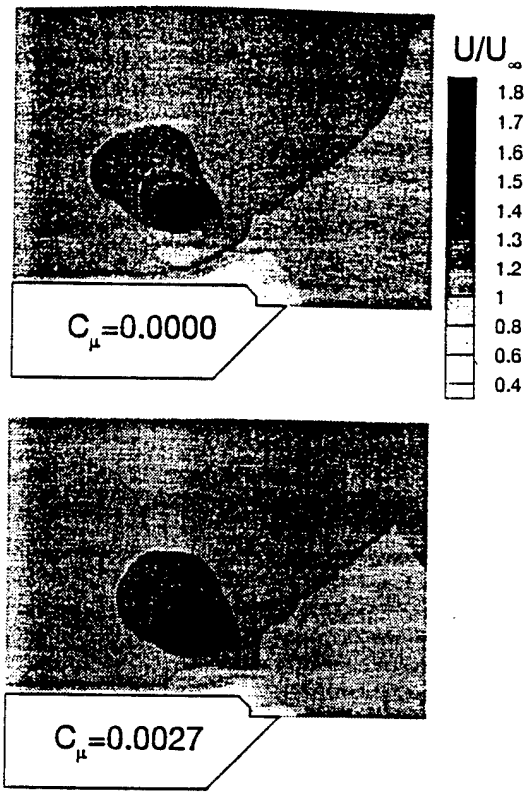

Fig. 11 Contours of normalized time-averaged axial velocity for C_μ = 0 and 0.0027, model B, Λ = 70 deg, α = 20 deg, and x/c = 0.6.

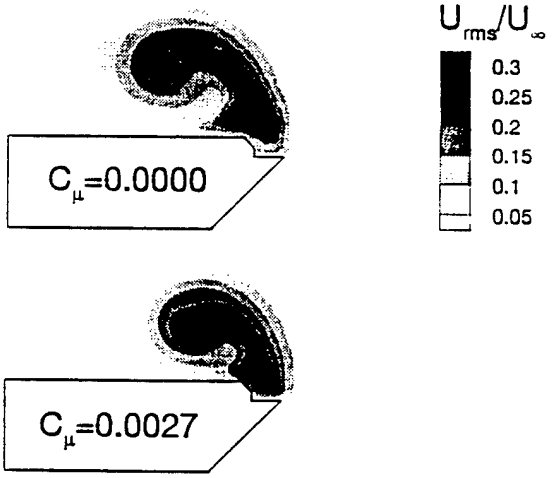

Fig. 12 Contours of normalized rms axial velocity C_μ = 0 and 0.0027, model B, Λ = 70 deg, α = 20 deg, and x/c = 0.6.

across the core is shown in Fig. 14. From these measurements of the velocity components, several parameters were estimated. The variation of maximum swirl angle with the suction coefficient is shown in Fig. 15a, which reveals a slight increase with increasing suction. The maximum axial vorticity (at the vortex axis) is shown as a function of suction coefficient in Fig. 15b, which indicates an initial increase followed by a slight decrease with increasing suction coefficient. In addition, the variation of circulation (obtained from the velocity measurements along the path shown in inset) is shown as a function of suction coefficient in Fig. 15c. This shows that overall circulation is not affected much with suction. In summary, for α = 20 deg, suction causes premature vortex breakdown for model B. This is caused by an increase in maximum swirl angle and maximum axial vorticity.

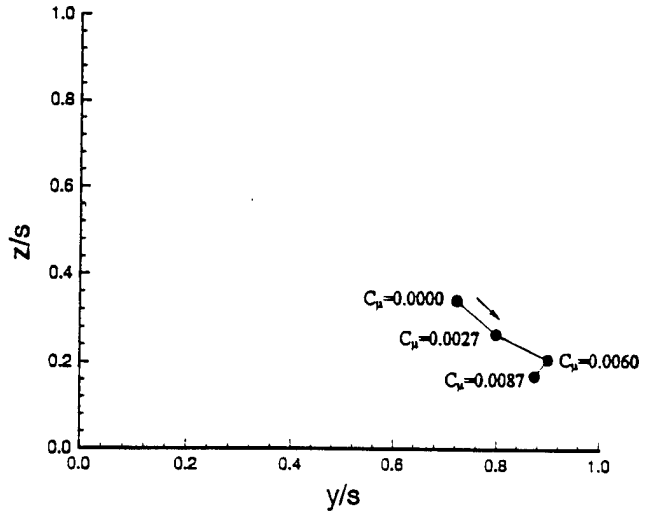

Fig. 13 Variation of location of vortex core, model B, Λ = 70 deg, α = 20 deg, and x/c = 0.6.

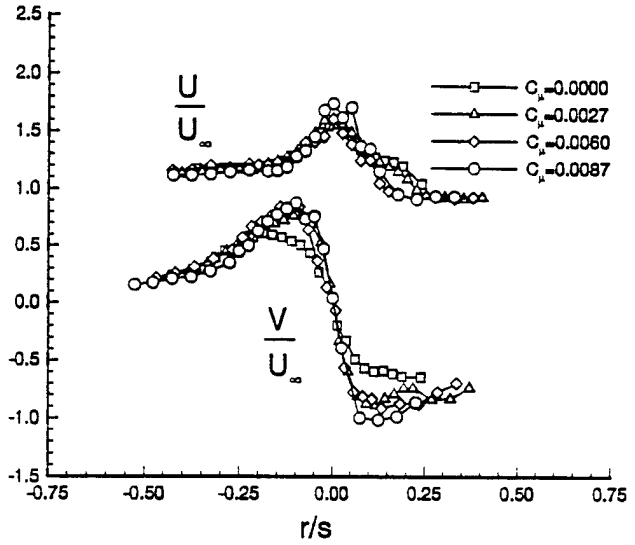

Fig. 14 Variation of axial and swirl velocity across the core, model B, Λ = 70 deg, α = 20 deg, and x/c = 0.6.

Discussion

Experiments using model A show that breakdown can be effectively moved downstream when suction is applied. Suction allows the shear layer to be manipulated at the point of separation along the leading edge. In this way, not only can the shear layer be vectored inboard and toward the wing surface, but also some of the vorticity can be removed before it enters the vortex core. This decrease in vorticity also causes the circulation and swirl angle to decrease. As a result, the vortex breakdown location moves downstream.

Experiments using model B show that breakdown moves upstream when suction is applied. Unlike model A, model B has the suction slot (sink) located inboard, away from the separated shear layer (see Fig. 1). The shear layer has already separated and begun its characteristic curvature over the wing surface before the suction slot of model B is encountered. This allows the vortex core to be manipulated while removing very little, if any, vorticity from the shear layer. Therefore, the vorticity fed into the shear layer does not change with suction. However, the shear layer can still be vectored inboard in a very effective way (with very small suction). The swirl velocity increases slightly as the separating shear layer is pulled tangentially by suction. The axial velocity component experiences very little change. The increasing swirl velocity component causes an increase in swirl angle that causes the breakdown location to move upstream.

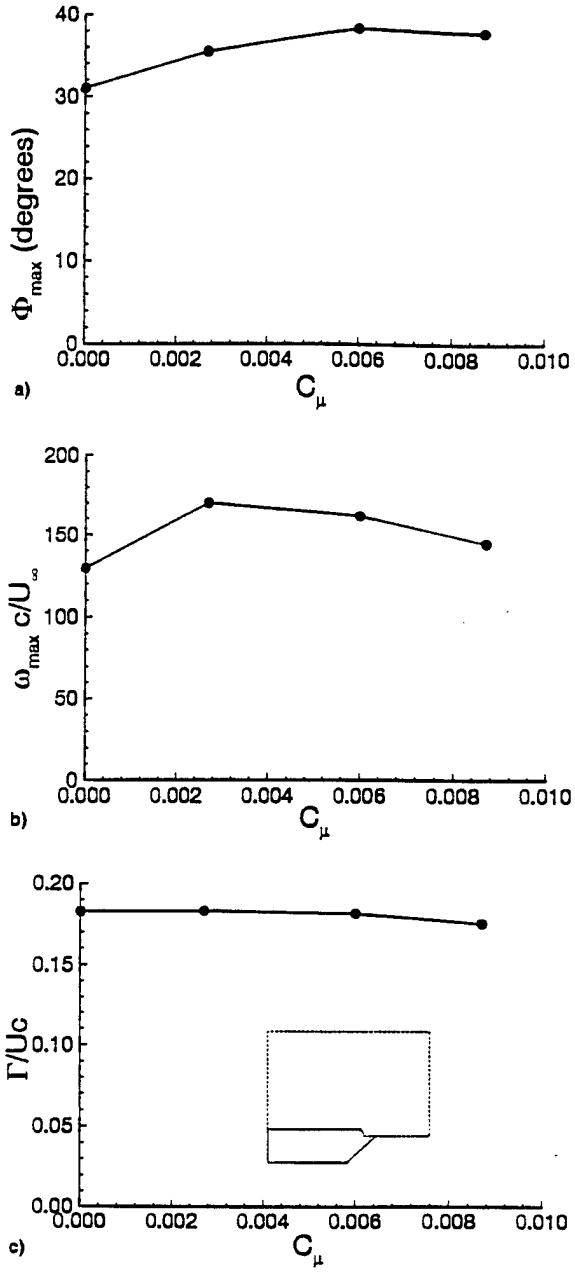

Fig. 15 Variation of a) maximum swirl angle, b) maximum axial vorticity, and c) circulation with suction coefficient, model B, Λ = 70 deg, α = 20 deg, and x/c = 0.6.

Conclusions

The effect of shear-layer control on leading-edge vortices over delta wings with sharp leading edges was investigated. By using suction near the separation point, the orientation of the shear layer could be modified. As a result, the structure of the leading-edge vortex and its location over the wing were modified as well. The maximum swirl angle in the core and overall circulation decreased with increasing suction. This caused the vortex breakdown location to move downstream. The geometry of the suction slot along the leading edge was found to be important. Use of a shorter plate on the upper surface of the wing caused the breakdown location to move upstream with suction. However, in this case, extremely small amounts of suction caused the location of the leading-edge vortex to change dramatically. This can be used to generate rolling moment over a delta wing. The leading-edge suction technique offers advantages over other methods, such as flaps,

by eliminating the need for moving surfaces and complicated mechanism. Thick rounded leading edges are not necessary.

Acknowledgments

This work was supported by the U.S. Air Force Office of Scientific Research Grant F49620-93-1-0516. The authors would like to thank Q. Deng for his help in the wind-tunnel experiments.

References

[1]Gursul, I., "Unsteady Flow Phenomena over Delta Wings at High Angle of Attack," *AIAA Journal*, Vol. 32, No. 2, 1994, pp. 225–231.

[2]Gursul, I., and Yang, H., "On Fluctuations of Vortex Breakdown Location," *Physics of Fluids*, Vol. 7, No. 1, 1995, pp. 229–231.

[3]Wood, N. J., Roberts, L., and Celik, Z., "Control of Asymmetric Vortical Flows over Delta Wings at High Angles of Attack," *Journal of Aircraft*, Vol. 27, No. 5, 1990, pp. 429–435.

[4]Gu, W., Robinson, O., and Rockwell, D., "Control of Vortices on a Delta Wing by Leading-Edge Injection," *AIAA Journal*, Vol. 31, No. 7, 1993, pp. 1177–1186.

[5]Spedding, G. R., Maxworthy, T., and Rignot, E., "Unsteady Vortex Flows over Delta Wings," *Proceedings of the 2nd AFOSR Workshop on Unsteady and Separated Flows* (Colorado Springs, CO), 1987, pp. 283–287.

[6]Karagounis, T., Maxworthy, T., and Spedding, G. R., "Generation and Control of Separated Vortices over a Delta Wing by Means of Leading Edge Flaps," AIAA Paper 89-0997, March 1989.

[7]Cheng, H. K., Edwards, R. H., Jia, Z. X., and Lee, C. J., "Vortex-Dominated Slender-Wing Problems Studied by a Point-Vortex Method," AIAA Paper 88-3744, 1988.

[8]Schaeller, N. W., Rediniotis, O. K., and Telionis, D. P., "Control of the Transient Development of Leading Edge Vortices by Vortex Cavity Flaps," AIAA Paper 94-1857, June 1994.

[9]Gursul, I., Yang, H., and Deng, Q., "Control of Vortex Breakdown with Leading-Edge Devices," AIAA Paper 95-0676, Jan. 1995.

[10]Bean, D., Greenwell, D. I., and Wood, N. J., "Vortex Control Technique for the Attenuation of Fin Buffet," *Journal of Aircraft*, Vol. 30, No. 6, 1993, pp. 847–853.

[11]Leu, T.-S., and Ho, C.-M., "Free Shear Layer Control and Its Application to Fan Noise," AIAA Paper 93-3242, July 1993.

[12]Hammond, D., and Redekopp, L. G., "Global Dynamics and Flow Vectoring in Asymmetric Wakes," AIAA Paper 94-2219, June 1994.

[13]Gad-el-Hak, M., and Blackwelder, R. F., "Control of the Discrete Vortices from a Delta Wing," *AIAA Journal*, Vol. 25, No. 8, 1987, pp. 1042–1049.

[14]McCormick, S., "Effect of Leading-Edge Suction on Vortices over Delta Wings," M.S. Thesis, Univ. of Cincinnati, Cincinnati, OH, 1995.

[15]Degani, D., "Effect of Splitter Plate on Unsteady Flows Around a Body of Revolution at Incidence," *Physics of Fluids A*, Vol. 3, No. 9, 1991, pp. 2122–2131.

[16]Schmucker, A., and Gersten, K., "Vortex Breakdown and Its Control on Delta Wings," *Fluid Dynamics Research*, Vol. 3, 1988, pp. 268–272.

[17]Cornelius, K. C., "Analysis of Vortex Bursting Utilizing Three-Dimensional Laser Measurements," *Journal of Aircraft*, Vol. 32, No. 2, 1995, pp. 297–306.

AIAA 96-0541

EFFECT OF SHEAR LAYER CONTROL ON LEADING EDGE VORTICES

S. McCormick and I. Gursul
University of Cincinnati
Cincinnati, OH

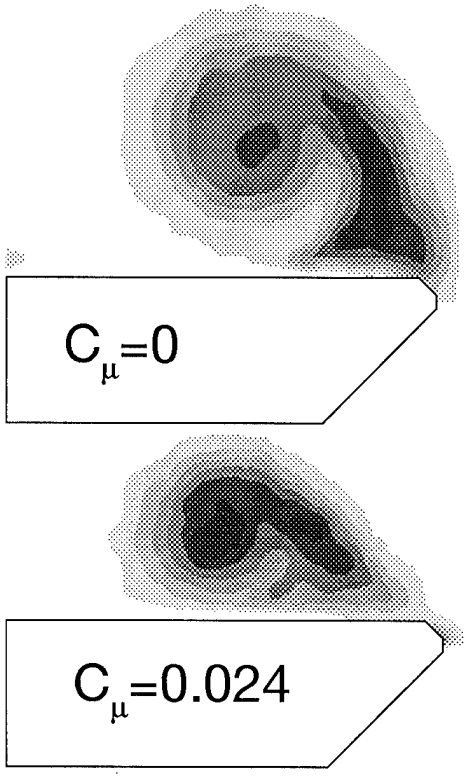

34th Aerospace Sciences
Meeting & Exhibit
January 15-18, 1996 / Reno, NV

EFFECT OF SHEAR LAYER CONTROL ON LEADING EDGE VORTICES

S. McCormick* and I. Gursul**

Department of Mechanical, Industrial and Nuclear Engineering
University of Cincinnati
Cincinnati, OH 45221-0072

Abstract

The effect of shear layer control on leading edge vortices over delta wings with *sharp* leading edges was investigated. By using suction near the separation point, the direction of the shear layer, and the location of the main vortex as well as its structure could be modified. At large angle of attack, vortex breakdown could be controlled as well.

Nomenclature

A_s	cross-sectional area of suction slot
c	chord length
C_μ	suction coefficient, $(V_s/U_\infty)^2(A_s/S)$
Re	Reynolds number
S	Surface area of the wing
s	local semispan
U_∞	free stream velocity
U	time-averaged axial velocity
u_{rms}	rms axial velocity
V	time-averaged swirl velocity
V_s	suction velocity
x	chordwise distance from the apex of the wing
x_{bd}	chordwise location of vortex breakdown
y	spanwise distance from wing root
z	distance above wing surface
α	angle of attack
Γ	circulation
ϕ	swirl angle, $\tan^{-1}$ V/U
Λ	sweep angle
ω	vorticity

---

* Graduate Student
** Assistant Professor

Introduction

Vortex breakdown phenomenon continues to be a challenging aspect of vortical flow fields. Since highly maneuverable aircraft are designed to operate at high angle of attack, vortex breakdown may move onto the wing and affect the stability of the aircraft. The unsteady characteristics[1,2] of the flow field after breakdown occurs is very important for stability and buffeting considerations.

Since the vorticity of the leading-edge vortices originates from the separation point along the leading edge, shear layer control can be used to influence the strength and structure of these vortices. Several efforts have been reported in this direction: blowing and suction in the tangential direction along a rounded leading-edge[3,4]; and use of leading-edge flaps[5-9]. The study of Wood et al. showed that a rounded, as opposed to a sharp, leading edge can alter the location of separation from the leading edge by tangential blowing as sketched in Figure 1. It has been pointed out that this technique uses the Coanda jet effect to help the shear layer attach to the convex surface[10]. Therefore, the application of this technique requires thick rounded leading edges. Leading-edge flaps are also known to be capable of controlling the separated shear layer and the leading edge vortices. Stationary as well as oscillating flaps have been studied with the control of vortex breakdown in mind[9].

One of the objectives of this work is to study the possibility of shear layer control over delta wings with sharp leading edges. In an attempt to control the development of a two-dimensional shear layer, Leu and Ho[11] applied suction at the trailing edge of a splitter plate as sketched in Figure 2a. It was shown that the free shear layer is sensitive to the modifications at the origin. The shear layer could be turned to a direction which is about 45 degrees from the streamwise direction. This type of "flow vectoring" was also studied by direct numerical simulations[12]. Gad-el-Hak and Blackwelder[13] applied periodic perturbations of injection and suction along the leading-edge of a delta wing. They found

maximum changes in the evolution of the shear layer when the frequency of perturbations is the subharmonic of the frequency of Kelvin-Helmholtz instability. However, no results were reported regarding the structure of the main vortex and the effect on vortex breakdown phenomenon. In this work, motivated by previous results, a similar shear layer control technique is explored. Suction is applied along the leading edge of a delta wing through a slot (see Figure 2b) and it is shown that the separated shear layer can be effectively manipulated. This, in turn, causes large modifications in the structure of the leading edge vortices. At large angle of attack, vortex breakdown can be controlled as well.

Experimental Facility

The majority of the experiments were carried out in a water channel with a cross-sectional area of 610 mm by 610 mm. The turbulence intensity in the water channel is 0.6%. Experiments were carried out for three different types of model delta wings (called Model A, B and C). In the water channel experiments, delta wings with sweep angles Λ=65° and 70° were tested. In Figure 3, the model delta wings are shown for Λ=70°. Model A is the basic delta wing, while Model B and C have shorter upper plates with different types of axial development (either parallel to the leading edge or conical). At the trailing edge of the wings, the span of the upper plate is 93.4% of the semispan. Since the shear layer turns inboard over the upper surface of the wing for the conventional wings, it was decided to study other configurations for which the upper plate is shorter and is not expected to interfere with the curved shear layer. The leading edges were beveled at 45 degrees on the windward side. The height of the suction slot is 1.8 mm. The chord lengths are c=254 mm for Λ=70° and c=203 mm for Λ=65°. The Reynolds number based on chord length was in the range of Re=40,000-50,000. The body of the models was made of Plexiglas and the upper plates were made of stainless steel.

Flow visualization of vortex breakdown was done by injecting fluid with food coloring dye near the apex of the models. The flow visualization was videotaped for further analysis. The velocity was measured with a single component laser Doppler velocimetry (LDV) system. The measurement volume was 0.1 mm in diameter and 0.81 mm in length. For axial velocity measurements, the velocity component parallel to the wing surface was measured. Since the measurements were taken parallel to the trailing edge (which is not perpendicular to the vortex axis), the velocity component approximately correspond to the axial velocity. Also, measurements of velocity component normal to the wing surface were taken in the plane containing the vortex core axis. As the measurements were taken along a traverse line parallel to the wing surface, the normal velocity approximately correspond to the swirl velocity across the vortex core. The traversing system used a minimum step of 1 mm which translated to a grid resolution of $\Delta y/s=\Delta z/s=0.0175$ at x/c=0.6. The measurement uncertainties for breakdown location and mean velocity were estimated as 0.4% and 1%, respectively.

Preliminary flow visualization experiments were carried out in a wind tunnel with a cross sectional area of 305 mm by 305 mm. The turbulence intensity in the wind tunnel was 0.25%. The model delta wings had a sweep angle of Λ=65°. The Reynolds number was around Re=12,000. Smoke injected near the apex helped to visualize the vortex core and provided information on vortex breakdown location.

The suction flow was generated by a pump or fan (for water channel and wind tunnel experiments) located outside the test section. The volume flow rate for suction was measured by a rotameter type flow meter. The dimensionless suction coefficient is defined as $C_\mu=(V_s/U_\infty)^2(A_s/S)$, where V_s is suction velocity at the suction slot, U_∞ is the free stream velocity, A_s is area of the suction slot, and S is the surface area of the wing. Further information regarding the experimental setup and instrumentation can be found in Reference 14.

Results

From the wind tunnel experiments for Λ=65°, the variation of breakdown location and vertical distance of vortex core above wing surface with suction coefficient is shown in Figure 4 for Models A and B. The fundamental difference in the response of Models A and B is that the breakdown location moves downstream for Model A whereas the breakdown location moves upstream for Model B. Also, for Model A, the breakdown location reaches a nearly constant level at larger values of the suction coefficient. Although suction causes the vortex core to get closer to wing surface for both models, the vortex core changes slightly with the suction coefficient for Model A while there is a large change of core location with small amounts of suction coefficient for Model B. In fact, similar amounts of change in the core location can be obtained with suction coefficients that are one order of magnitude smaller for Model B than for Model A.

From the water channel experiments for Λ=70°, the variation of breakdown location with suction coefficient is shown in Figure 5 for Models A, B, and C. The results are qualitatively similar to those presented in Figure 4. Moreover, the response of Models B and C are qualitatively similar. For Model A, the effect of suction on breakdown is generally positive, except at very large angle attack where suction does not make much difference. For α=30°, the breakdown location reaches a maximum around C_μ=0.024 after which it becomes nearly constant. Detailed LDV measurements were carried out for α=30°.

The constant contours of the normalized time-averaged axial velocity for x/c=0.6 (upstream of the breakdown location) are compared in Figure 6 for C_μ=0 and C_μ=0.024 at which the breakdown location is at maximum downstream location. It is clear that the vortex core moves inboard and closer to the wing surface. There is also a slight decrease in the maximum axial velocity with suction. The constant contours of the normalized rms axial velocity are compared in Figure 7 for C_μ=0 and C_μ=0.024. The shape of the rms velocity contours is a good indicator of the shear layer and main vortex. (This was also shown for vortical flows over a body of revolution at incidence[15]. The high rms velocity fluctuations indicated the location of the vortex cores. The rms velocity contours were found to be representative of the cross sections of the tip vortices). In the present experiments, very large levels of rms velocity (up to 30% of the free stream velocity) in the shear layer and in the core of the leading edge vortex were observed. It should be noted that this high turbulence level is observed well upstream of the breakdown location. Other experiments in vortical flows (in the absence of breakdown) showed very high levels of turbulence[15-17]. This is not very surprising if the dynamics of the shear layer is considered (i.e., development of coherent structures and pairing etc.). Although high level of turbulence intensity was reported in the vortex cores previously for large Reynolds numbers, the existence of high levels was not known for relatively low Reynolds numbers (based on the chord length) such as Re=50,000. It is clear from Figure 7 that, with suction, the direction of the shear layer is changed. It is also evident that the vortex core moves inboard and toward the wing surface with suction.

Since suction was applied along the one leading edge, its effect on the other vortex was investigated[14]. Time-averaged axial velocity and rms axial velocity contours (not shown here due to space limitations) revealed that there was no change in the structure of the other vortex. Therefore, suction can be used for independent control of leading edge vortices by generating a net rolling moment.

The constant contours of the normalized time-averaged axial velocity for x/c=1.0 (downstream of the breakdown location in the absence of suction) are compared in Figure 8 for C_μ=0 and C_μ=0.024. Without suction, the flow retardation which is characteristic of breakdown is visible. The time-averaged axial velocity in the core drops to near zero values, and the size of the core increases greatly. With the suction, the axial velocity becomes jet-like and the core location gets closer to the wing. The constant contours of the normalized rms axial velocity are compared in Figure 9 for C_μ=0 and C_μ=0.024. With the suction, a decrease in the maximum rms velocity in the core is observed due to the delay of the vortex breakdown. The change in the core location is also evident. In Figure 10, the variation of swirl velocity across the core is shown for suction and no suction. It is seen that the size of the vortex core decreases and the axial vorticity increases with the suction (as evidenced by the change in the slope), which is consistent with the changes associated with the movement of breakdown location downstream of the measurement plane.

In order to quantify the effect of suction on upstream conditions (before breakdown) and on the parameters affecting breakdown, detailed measurements were taken at x/c=0.6 for several values of the suction coefficient. The location of vortex core was found by locating the position of the maximum of the axial velocity distribution (at x/c=0.6, upstream of breakdown location). Then, measurements of axial and swirl velocity components were taken across the vortex core. The variation of location of the vortex core is shown in Figure 11. It is seen that the vortex core moves slightly inboard and closer to the wing surface with increasing suction coefficient. However, with increasing suction coefficient, the changes in the core location becomes relatively small. The variation of axial and swirl velocities across the core is shown in Figure 12. A decrease in the maximum axial velocity is observed with increasing suction. The maximum values of the swirl velocity also decrease with increasing suction. Slightly outboard of the core, a decrease and then a local maximum are observed (due to the shear layer), followed by a leveling of the swirl velocity. Based on the measured axial and swirl velocity components, the swirl angle ($\phi=\tan^{-1}$ V/U) can be calculated as a function of the distance from the vortex axis. The variation of swirl angle with the distance from the vortex axis is given in detail in

Reference 14. The swirl angle is zero at the center of the vortex core and reaches a maximum at the edge of the subcore (the subcore being the region where most of the streamwise vorticity is confined). The variation of maximum swirl angle with the suction coefficient is shown in Figure 13a. It is seen that there is a decrease in swirl angle with increasing suction coefficient although the changes become more gradual at larger values of the suction coefficient. The axial vorticity distribution can also be calculated assuming rotational symmetry. In other words, the swirl velocity profile is sufficient to estimate the axial vorticity. The axial vorticity component is given by $\omega=\partial V/\partial r+V/r$. An example of the calculated vorticity distribution (by the forward differencing method) is given in Reference 14. The maximum axial vorticity (which occurs at the vortex axis) is shown as a function of suction coefficient in Figure 13b. A decrease in the maximum axial velocity with suction is observed. However, there is almost no change with further changes in the suction coefficient. In addition, the variation of circulation (obtained from the velocity measurements along the path shown in inset) is shown as a function of suction coefficient in Figure 13c. The overall circulation decreases with increasing suction coefficient. Although this closed contour encloses the main vortex, secondary vortex, and shear layer, it is a reasonable indicator of the strength of the main vortex. Moreover, the circulation calculated this way can be interpreted as the rate at which vorticity is fed. In summary, it is shown that, for $\alpha=30°$, suction delays the vortex breakdown for Model A. This is due to a decrease in maximum swirl angle and circulation as well as in maximum axial vorticity. Further experiments for $\Lambda=65°$ also showed similar results[14].

For Model B and C, the flow visualization showed an opposite trend for the variation of breakdown location with suction (see Figure 5). Therefore, it was decided to carry out detailed measurements for Model B at $\alpha=20°$. The constant contours of the normalized time-averaged axial velocity for x/c=0.6 (upstream of the breakdown location) are compared in Figure 14 for $C_\mu=0$ and $C_\mu=0.0027$. It is seen that an extremely small amount of suction (almost one-tenth of the amount used for Model A) is sufficient to displace the vortex core. There is a slight increase in the maximum axial velocity. The constant contours of the normalized rms axial velocity shown in Figure 15 indicate that the vortex core moves outboard and closer to the wing surface with suction. Higher levels of rms axial velocity are found in the core when suction is applied.

The location of vortex core was found from the axial velocity distributions (at x/c=0.6, upstream of breakdown location). The variation of location of vortex core is shown in Figure 16. It is seen that, initially, the vortex core moves outboard and closer to the wing surface with increasing suction coefficient. There is a small inboard displacement for the largest suction coefficient. The variation of axial and swirl velocities across the core is shown in Figure 17. From these measurements of the velocity components, several parameters were estimated. The variation of maximum swirl angle with the suction coefficient is shown in Figure 18a, which reveals a slight increase with increasing suction. The maximum axial vorticity (at the vortex axis) is shown as a function of suction coefficient in Figure 18b, which indicates an initial increase followed by a slight decrease with increasing suction coefficient. In addition, the variation of circulation (obtained from the velocity measurements along the path shown in inset) is shown as a function of suction coefficient in Figure 18c. This shows that overall circulation is not affected much with suction. In summary, for $\alpha=20°$, suction causes premature vortex breakdown for Model B. This is due to an increase in maximum swirl angle and maximum axial vorticity.

Discussion

Experiments using Model A show that breakdown can be effectively moved downstream when suction is applied. Suction allows the shear layer to be manipulated at the point of separation along the leading edge. In this way, not only can the shear layer be "vectored" inboard and toward the wing surface, but also some of the vorticity can be removed before it enters the vortex core. This decrease in vorticity also causes the circulation and swirl angle to decrease. As a result, the vortex breakdown location moves downstream.

Experiments using Model B show that breakdown moves upstream when suction is applied. Unlike Model A, Model B has the suction slot ("sink") located inboard, away from the separated shear layer. Figure 19 shows schematically the point where suction is applied for Model A and B. The shear layer has already separated and begun its characteristic curvature over the wing surface before the suction slot of Model B is encountered. This allows the vortex core to be manipulated while removing very little, if any, vorticity from the shear layer. Therefore, the vorticity fed into the shear layer does not change with suction. However, the shear layer can still be "vectored" inboard in a very effective way (with very

small suction). The swirl velocity increases slightly as the separating shear layer is pulled tangentially by suction. The axial velocity component experiences very little change. The increasing swirl velocity component causes an increase in swirl angle which causes the breakdown location to move upstream.

Conclusions

The effect of shear layer control on leading edge vortices over delta wings with sharp leading edges was investigated. By using suction near the separation point, the orientation of the shear layer could be modified. As a result, the structure of the leading edge vortex and its location over the wing were modified as well. The maximum swirl angle in the core and overall circulation decreased with increasing suction. This caused the vortex breakdown location to move upstream. The geometry of the suction slot along the leading edge was found to be important. Use of a shorter plate on the upper surface of the wing caused the breakdown location to move upstream with suction. However, in this case, extremely small amounts of suction caused the location of the leading edge vortex to change dramatically. This can be used to generate rolling moment over a delta wing.

Acknowledgment

This work was supported by the Air Force Office of Scientific Research Grant No. F49620-93-1-0516. The authors would like to thank to Q. Deng for his help in the wind tunnel experiments.

List of References

1. Gursul, I. "Unsteady Flow Phenomena over Delta Wings at High Angle of Attack", *AIAA Journal*, vol. 32, no. 2, February 1994, pp. 225-231.

2. Gursul, I and Yang, H., "On Fluctuations of Vortex Breakdown Location", *Physics of Fluids*, 7 (1), 229, (1995).

3. Wood, N.J., Roberts, L. and Celik, Z., "Control of Asymmetric Vortical Flows over Delta Wings at High Angles of Attack", *Journal of Aircraft*, vol. 27, no. 5, pp. 429-435, (1990).

4. Gu, W., Robinson, O. and Rockwell, D., "Control of Vortices on a Delta Wing by Leading-Edge Injection", *AIAA Journal*, vol. 31, no. 7, July 1993, pp. 1177-1186.

5. Spedding, G.R., Maxworthy, T. and Rignot, E., "Unsteady Vortex Flows over Delta Wings", Proc. of 2nd AFOSR Workshop on Unsteady and Separated Flows, Colorado Springs, July 1987, pp. 283-287.

6. Karagounis, T., Maxworthy, T. and Spedding, G.R., "Generation and Control of Separated Vortices over a Delta Wing by Means of Leading Edge Flaps", AIAA Paper 89-0997, AIAA 2nd Shear Flow Conference, March 13-16, 1989, Tempe, AZ.

7. Cheng, H.K., Edwards, R.H., Jia, Z.X. and Lee, C.J., "Vortex-Dominated Slender-Wing Problems Studied by a Point-Vortex Method", AIAA-88-3744, 1988.

8. Schaeller, N.W., Rediniotis, O.K. and Telionis, D.P., "Control of the Transient Development of Leading Edge Vortices by Vortex Cavity Flaps", AIAA-94-1857, 25th AIAA Fluid Dynamics Conference, June 20-23, 1994, Colorado Springs, CO.

9. Gursul, I., Yang, H. and Deng, Q., "Control of Vortex Breakdown with Leading-Edge Devices", AIAA Paper 95-0676, 33rd Aerospace Sciences Meeting and Exhibit, January 9-12, 1995, Reno, NV.

10. Bean, D., Greenwell, D.I. and Wood, N.J., "Vortex Control Technique for the Attenuation of Fin Buffet", *Journal of Aircraft*, vol. 30, no. 6, pp. 847-853, 1993.

11. Leu, T-S. and Ho, C-M., "Free Shear Layer Control and its Application to Fan Noise", AIAA Paper 93-3242, AIAA Shear Flow Conference, July 6-9, 1993, Orlando, FL.

12. Hammond , D. and Redekopp, L.G., "Global Dynamics and Flow Vectoring in Asymmetric Wakes", AIAA Paper 94-2219, 25th AIAA Fluid Dynamics Conference, June 20-23, 1994, Colorado Springs, CO.

13. Gad-el-Hak, M. and Blackwelder, R.F., "Control of the Discrete Vortices from a Delta Wing", *AIAA Journal*, vol. 25, no. 8, 1987, pp. 1042-1049.

14. McCormick, S., "Effect of Leading-Edge Suction on Vortices over Delta Wings", M.S. Thesis, University of Cincinnati, 1995.

15. Degani, D. "Effect of splitter plate on unsteady flows around a body of revolution at incidence", *Physics of Fluids A*, vol. 3, no. 9, pp. 2122-2131, 1991.

16. Schmucker, A. and Gersten, K., "Vortex Breakdown and its Control on Delta Wings", *Fluid Dynamics Research*, vol. 3, pp. 268-272, 1988.

17. Cornelius, K.C., "Analysis of Vortex Bursting Utilizing Three-Dimensional Laser Measurements", *Journal of Aircraft*, vol. 32, no.2, 1995, pp. 297-306.

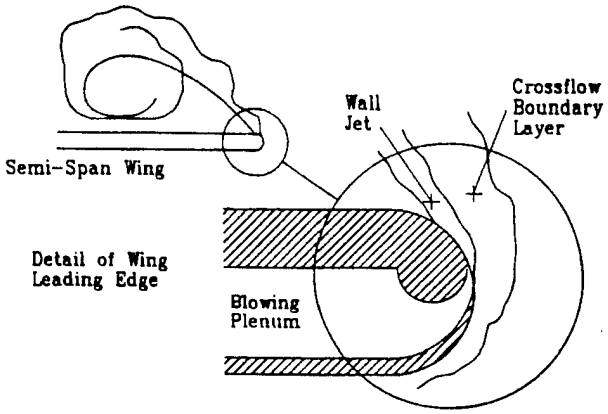

Figure 1: Tangential blowing from a rounded leading edge (Wood et al. 1990).

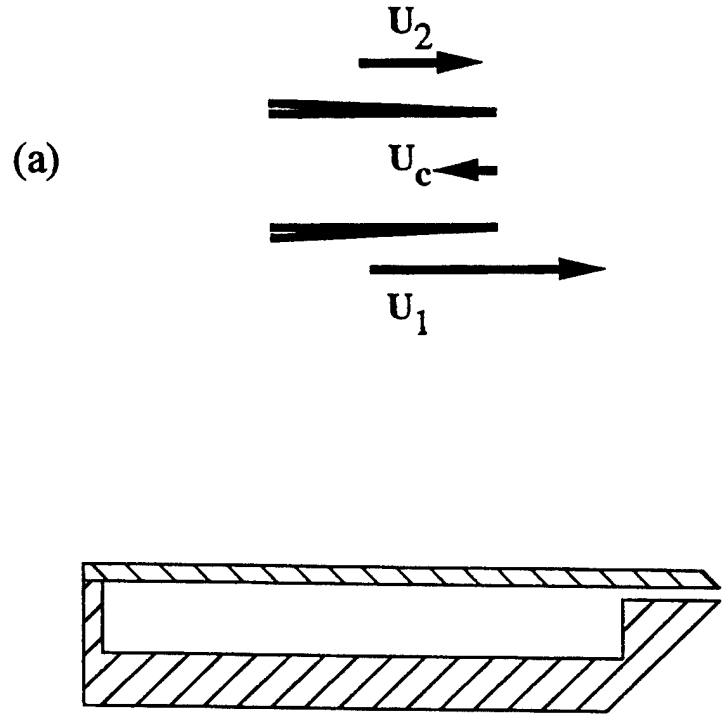

Figure 2: (a) Shear layer control of a two-dimensional mixing layer by suction (Leu and Ho 1993); (b) geometry of delta wing with suction slot.

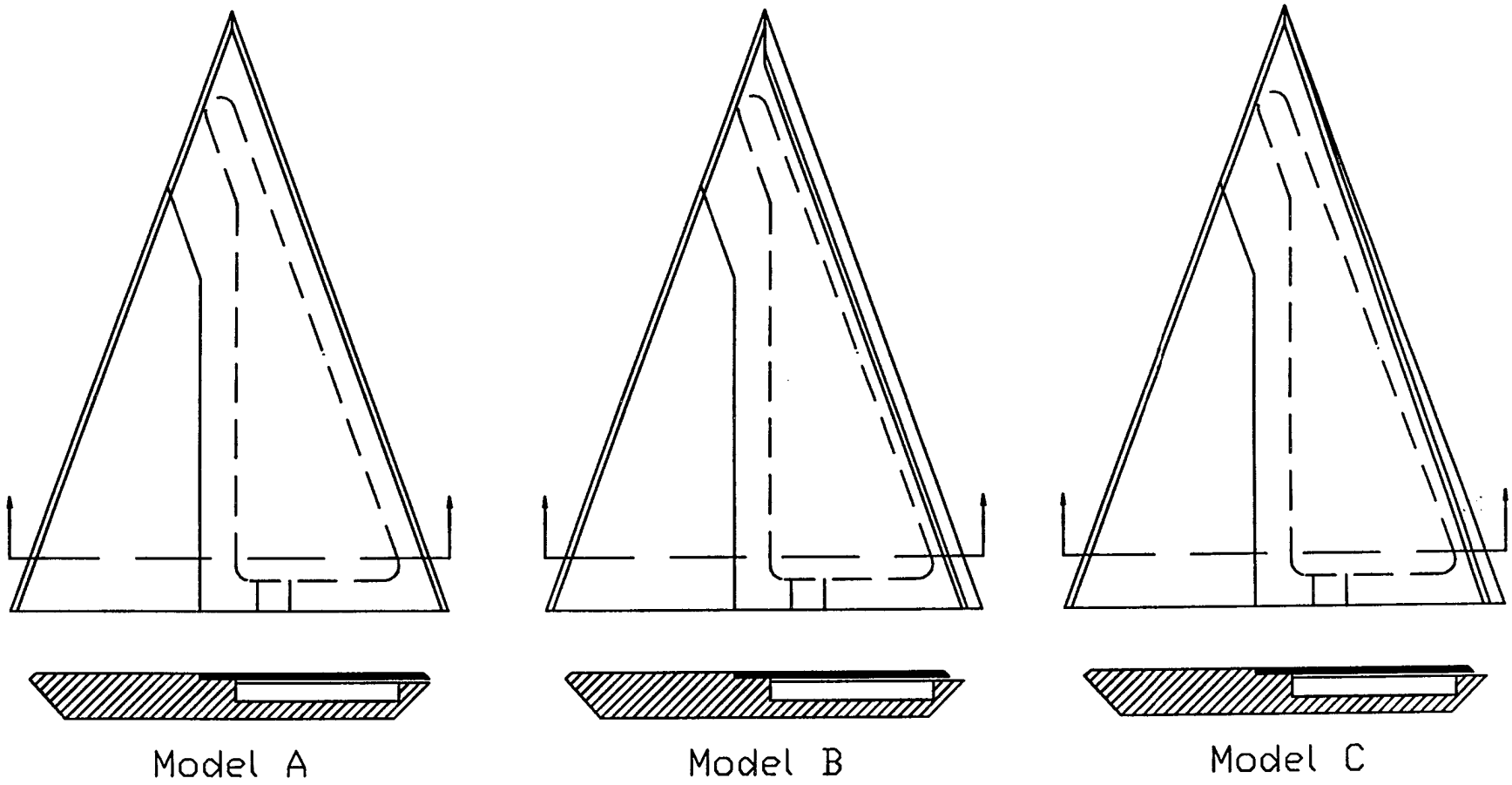

Figure 3: Three different type of model delta wings for Λ=70°.

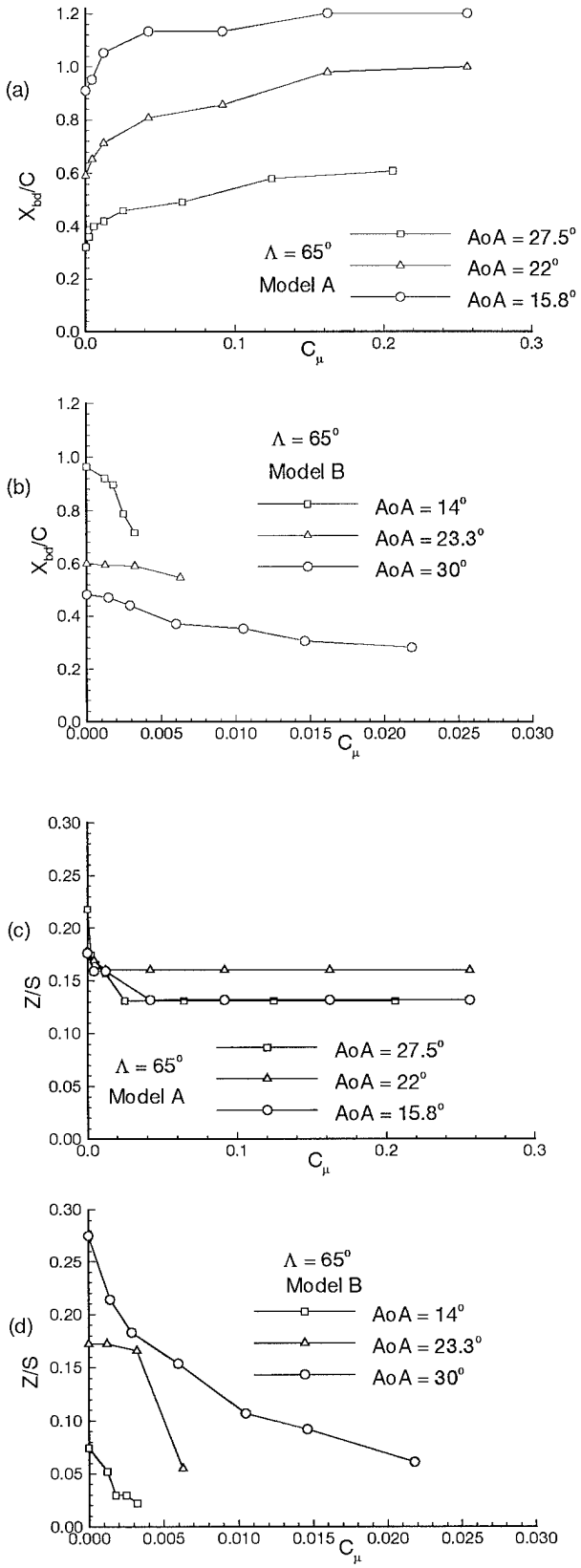

Figure 4: Variation of breakdown location with suction coefficient for (a) Model A, (b) Model B; variation of vertical distance of vortex core above wing surface with suction coefficient for (c) Model A, (d) Model b, Λ=65°.

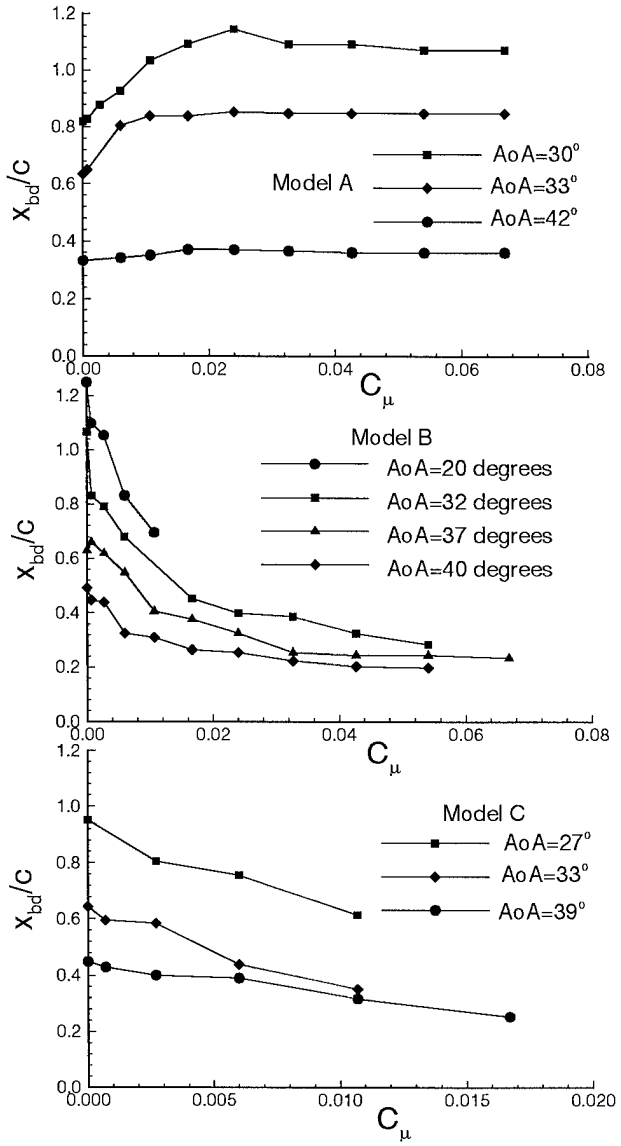

Figure 5: Variation of breakdown location with suction coefficient for Models A, B, and C, Λ=70°.

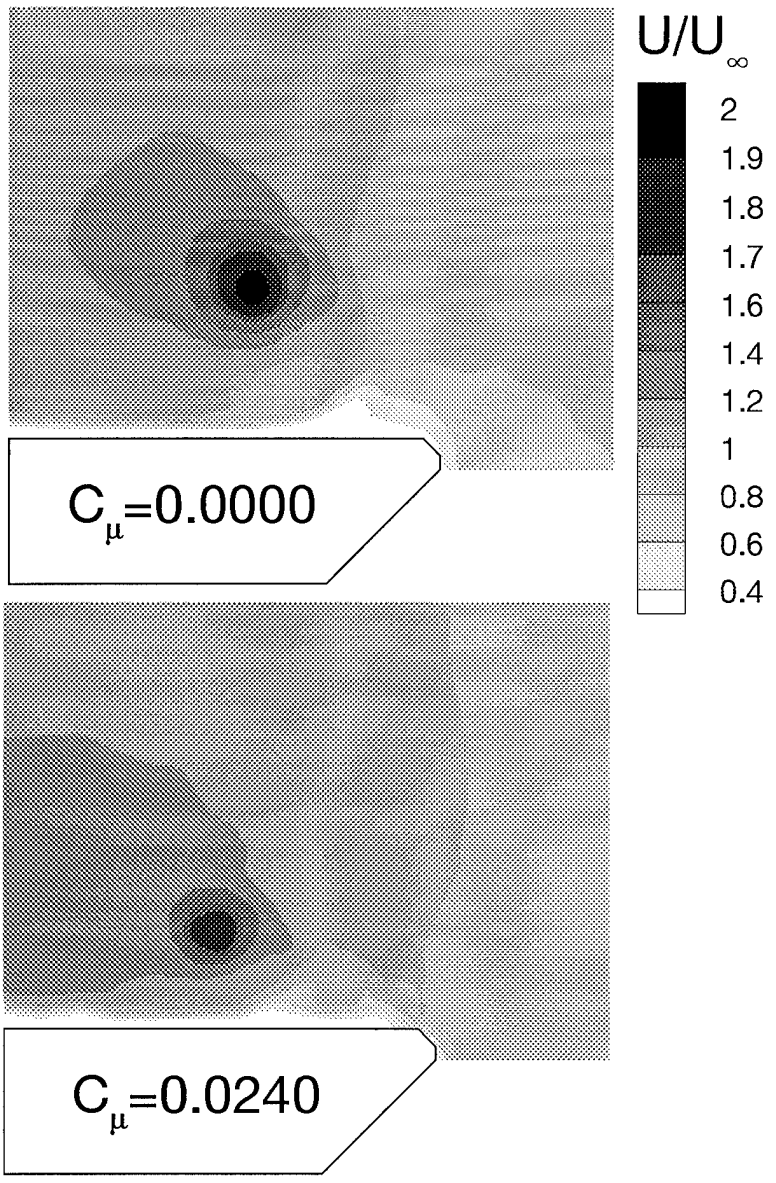

Figure 6: Contours of normalized time-averaged axial velocity for C_μ=0 and C_μ=0.024, Model A, Λ=70°, α=30°, x/c=0.6.

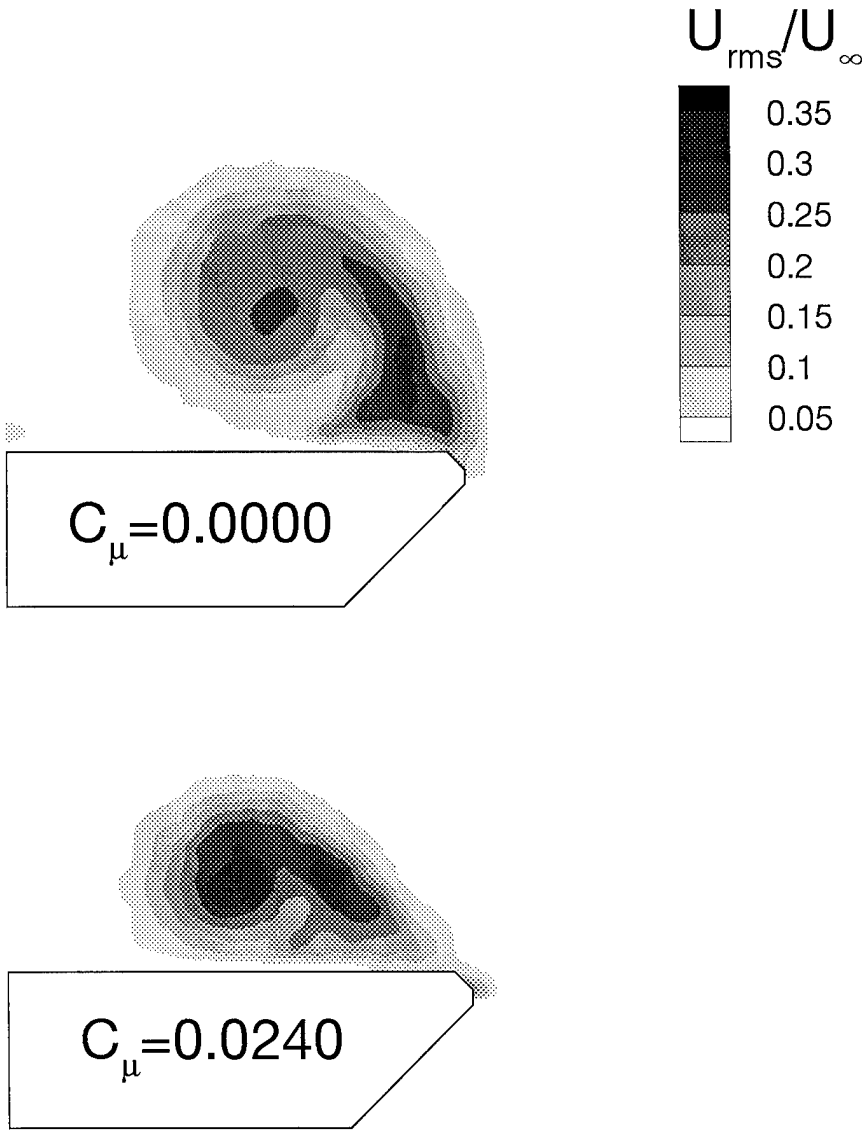

Figure 7: Contours of normalized rms axial velocity C_μ=0 and C_μ=0.024, Model A, Λ=70°, α=30°, x/c=0.6.

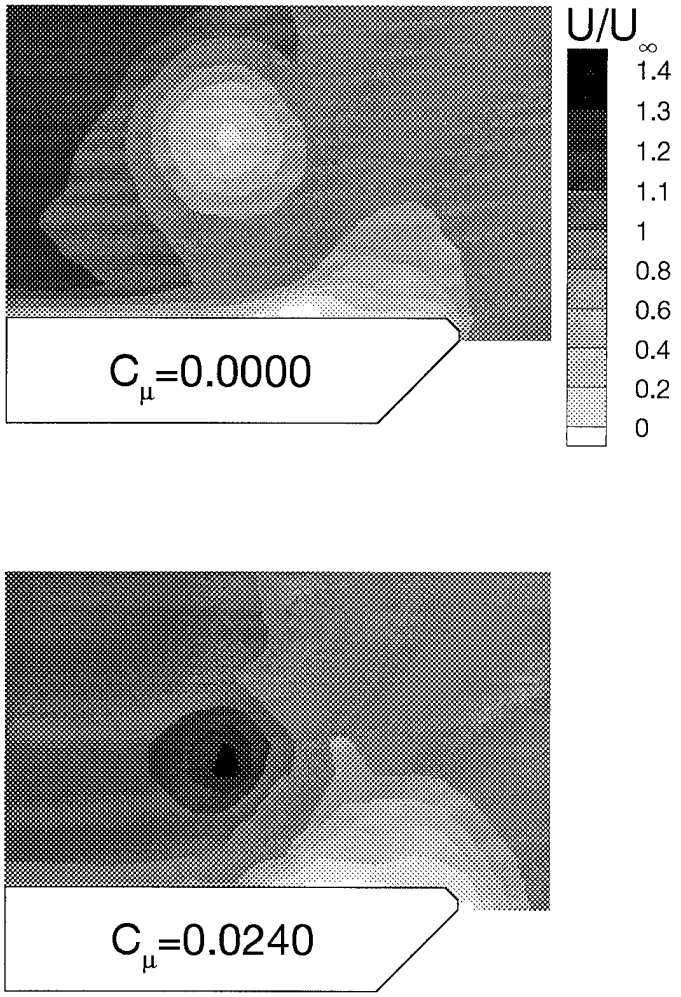

Figure 8: Contours of normalized time-averaged axial velocity for C_μ=0 and C_μ=0.024, Model A, Λ=70°, α=30°, x/c=1.0.

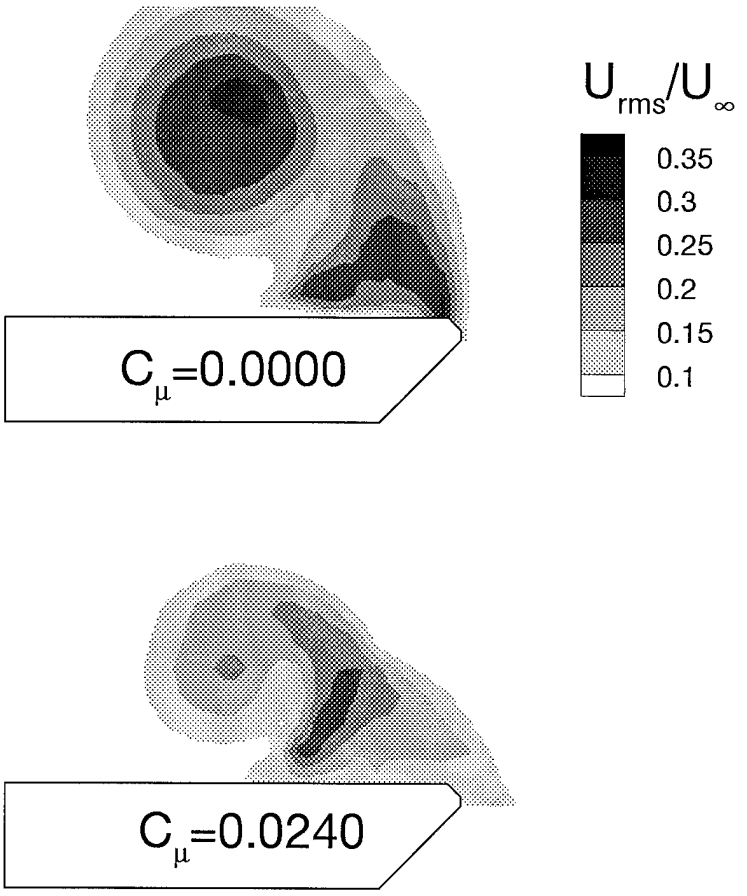

Figure 9: Contours of normalized rms axial velocity for C_{μ}=0 and C_{μ}=0.024, Model A, Λ=70°, α=30°, x/c=1.0.

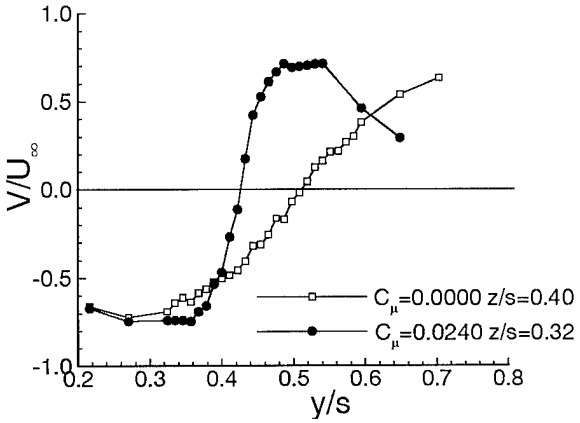

Figure 10: Variation of swirl velocity across the core for C_μ=0 and C_μ=0.024, Model A, Λ=70°, α=30°, x/c=1.0.

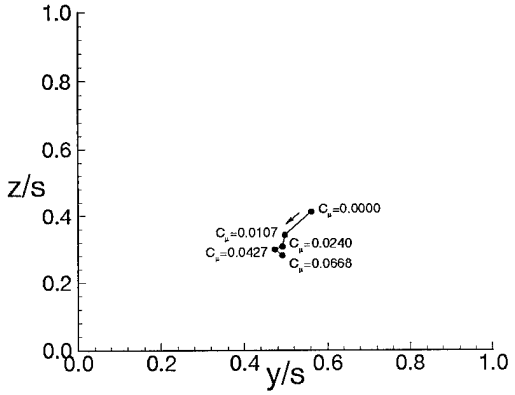

Figure 11: Variation of location of vortex core, Model A, Λ=70°, α=30°, x/c=0.6.

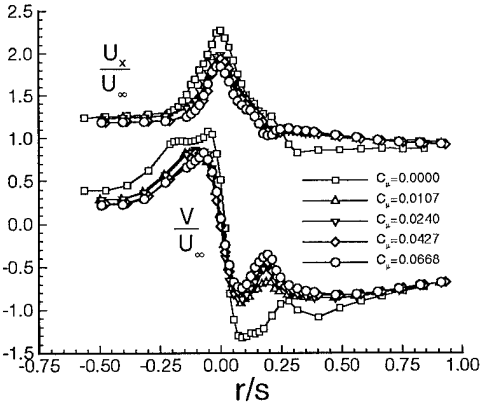

Figure 12: Variation of axial and swirl velocity across the core, Model A, Λ=70°, α=30°, x/c=0.6.

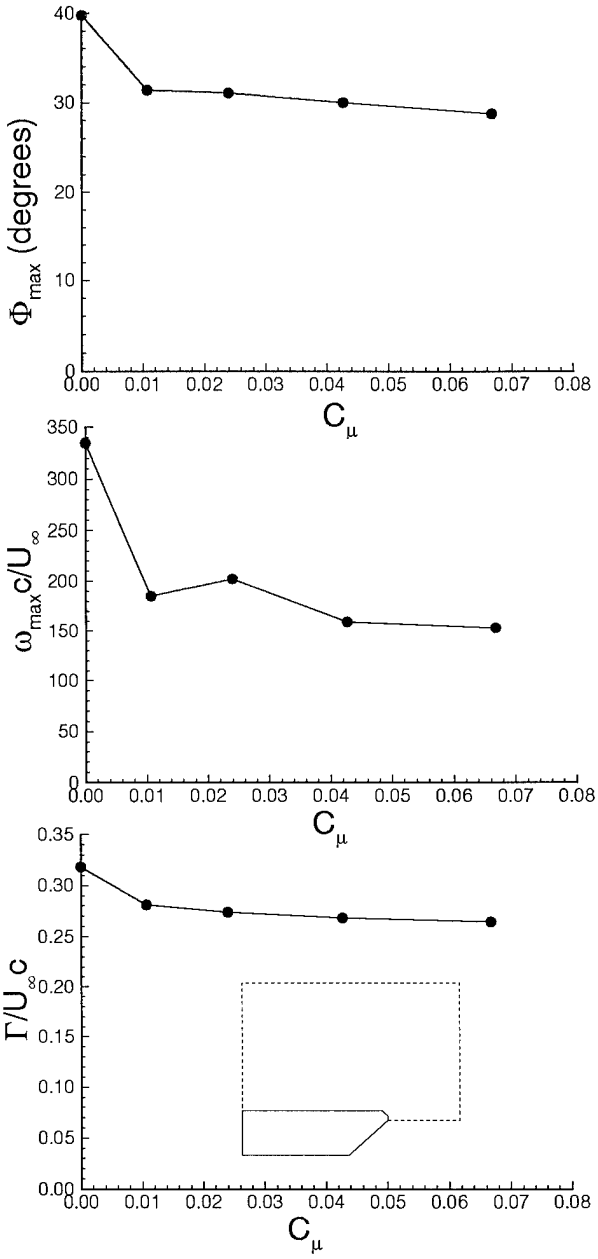

Figure 13: Variation of (a) maximum swirl angle, (b) maximum axial vorticity, (c) circulation with suction coefficient, Model A, Λ=70°, α=30°, x/c=0.6.

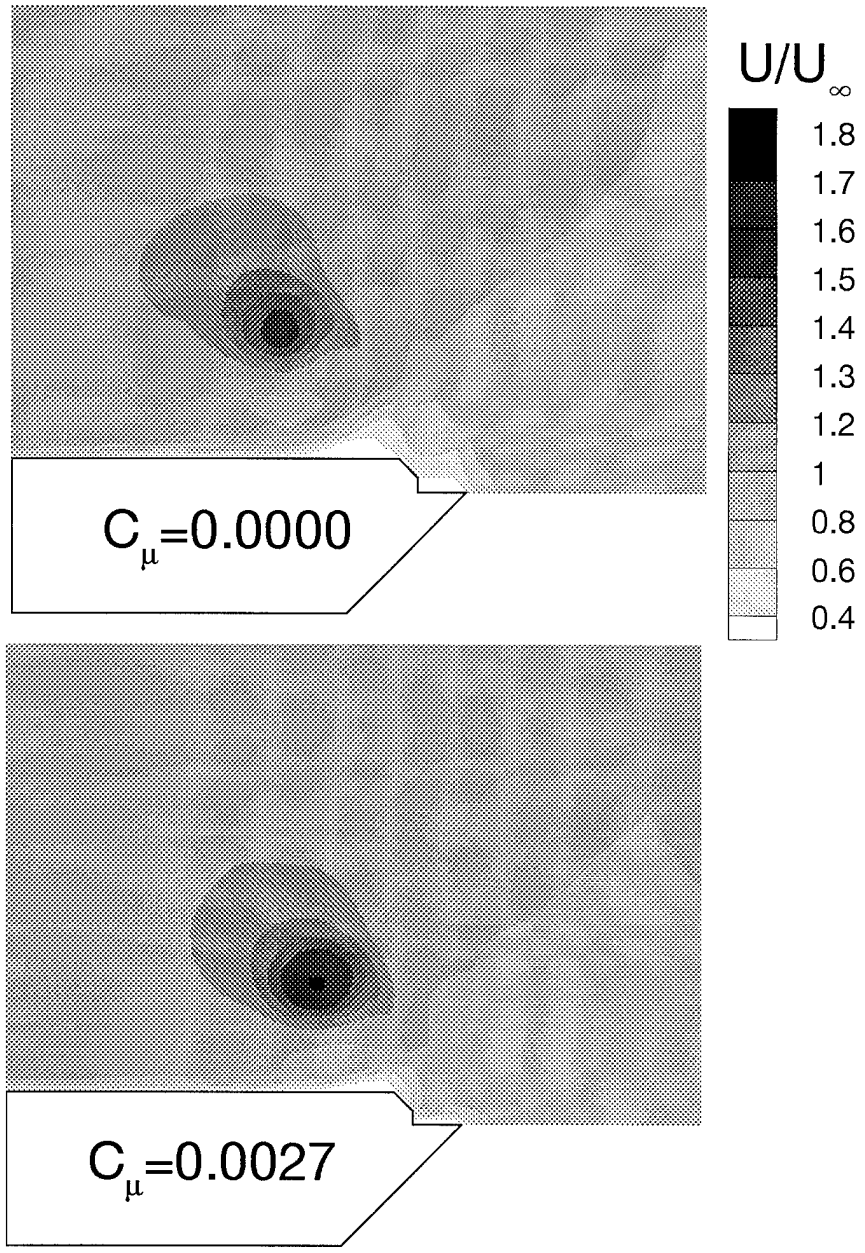

Figure 14: Contours of normalized time-averaged axial velocity for C_μ=0 and C_μ=0.0027, Model B, Λ=70°, α=20°, x/c=0.6.

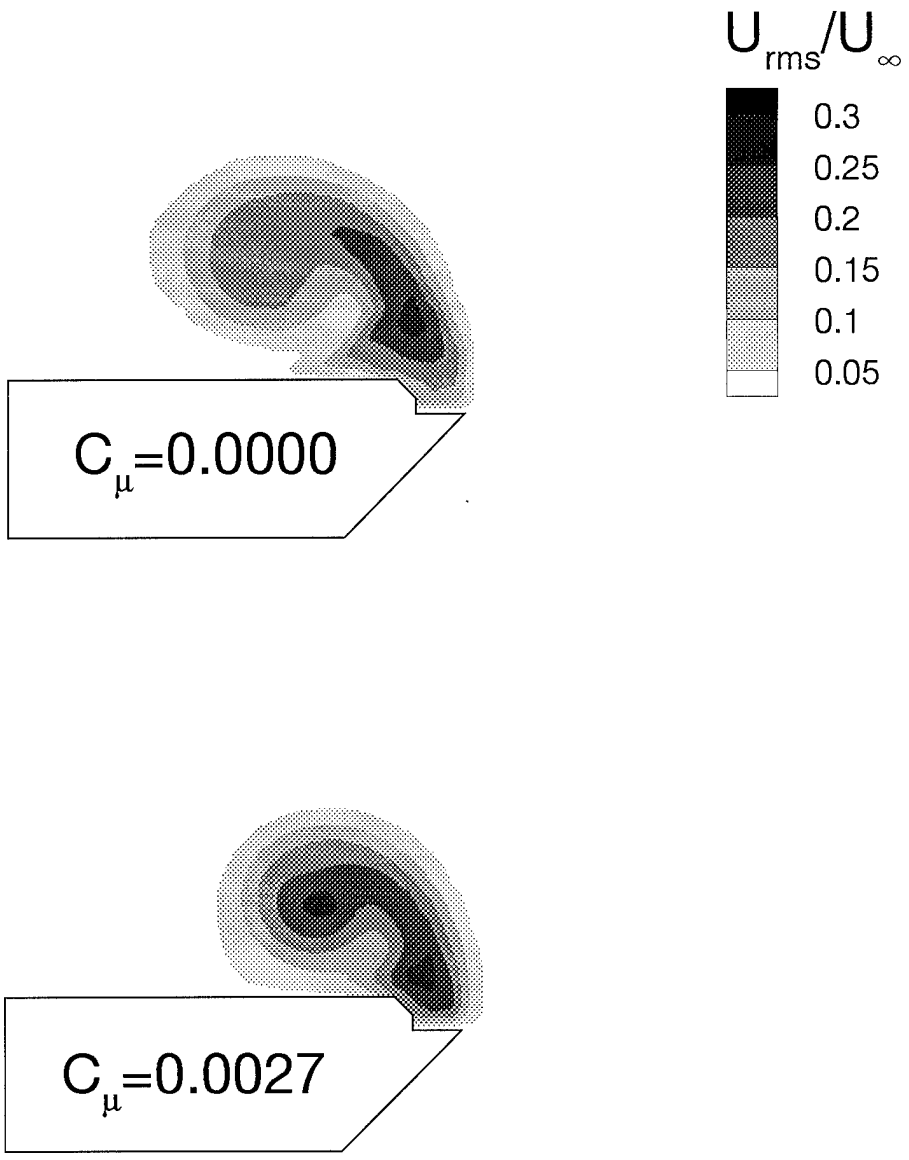

Figure 15: Contours of normalized rms axial velocity for C_{μ}=0 and C_{μ}=0.0027, Model B, Λ=70°, α=20°, x/c=0.6.

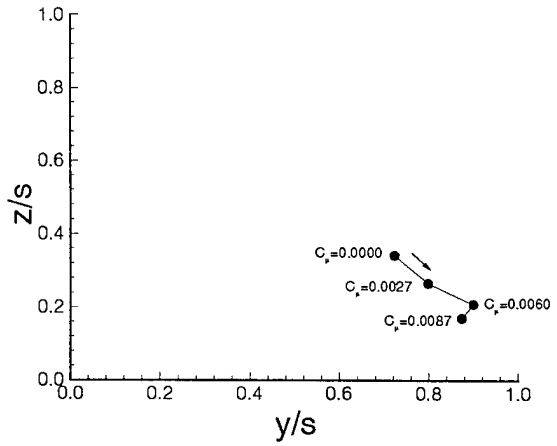

Figure 16: Variation of location of vortex core, Model B, Λ=70°, α=20°, x/c=0.6.

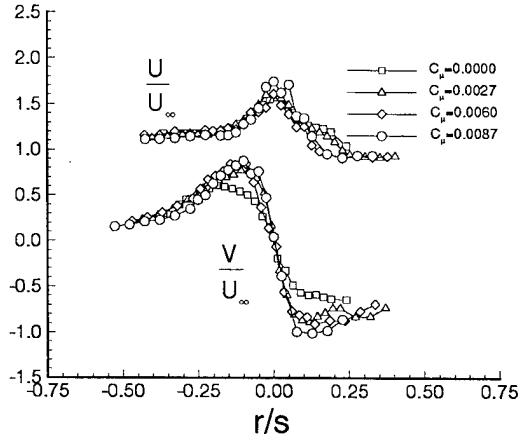

Figure 17: Variation of axial and swirl velocity across the core, Model B, Λ=70°, α=20°, x/c=0.6.

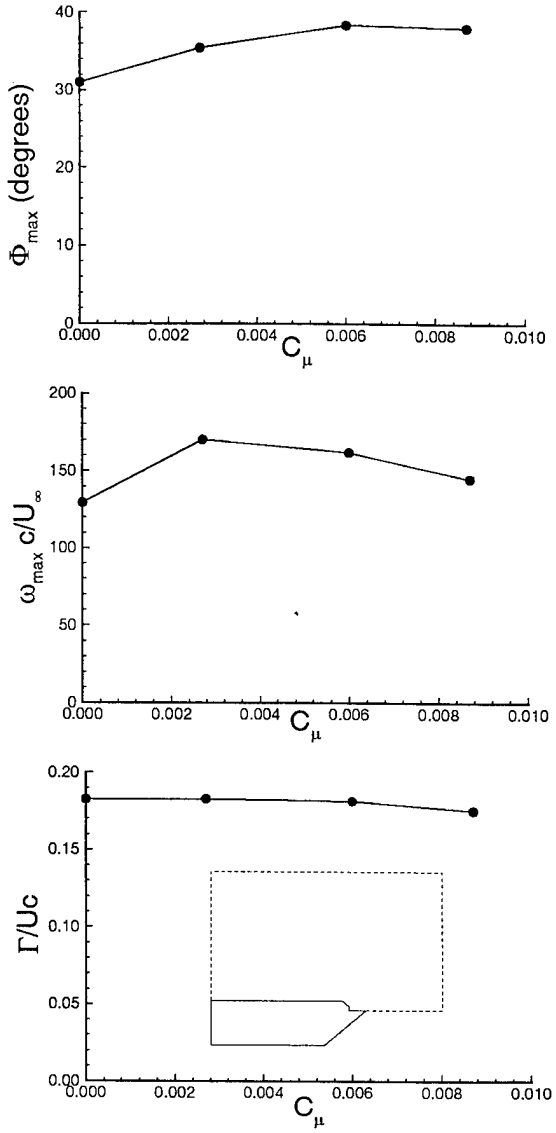

Figure 18: Variation of (a) maximum swirl velocity, (b) maximum axial vorticity, (c) circulation with suction coefficient, Model B, Λ=70°, α=20°, x/c=0.6.

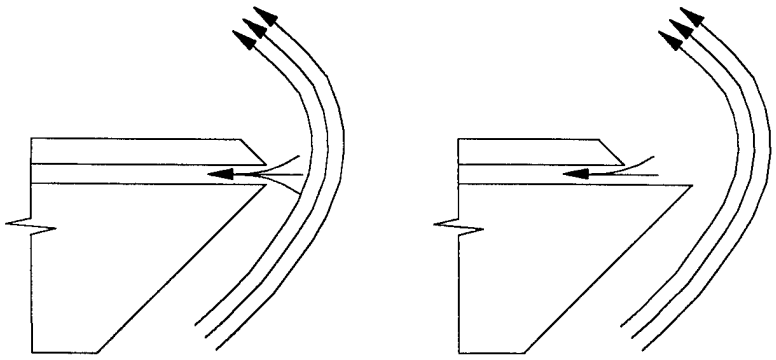

Figure 19: Close up of suction slot with shear layer for (a) Model A, and (b) Model B.